

# Analysis of nucleotides by pressure-assisted capillary electrophoresis–mass spectrometry using silanol mask technique

Tomoyoshi Soga<sup>a,b,\*</sup>, Takamasa Ishikawa<sup>b</sup>, Saori Igarashi<sup>a</sup>,  
Kaori Sugawara<sup>a</sup>, Yuji Kakazu<sup>a</sup>, Masaru Tomita<sup>a,b</sup>

<sup>a</sup> Institute for Advanced Biosciences, Keio University, Kakuganji, Tsuruoka, Yamagata 997-0052, Japan

<sup>b</sup> Human Metabolome Technologies Inc., Kakuganji, Tsuruoka, Yamagata 997-0052, Japan

Available online 18 May 2007

## Abstract

A method for the determination of nucleotides based on pressure-assisted capillary electrophoresis–electrospray ionization mass spectrometry (PACE–MS) is described. To prevent multi-phosphorylated species from adsorbing onto the fused-silica capillary, silanol groups were masked with phosphate ions by preconditioning the capillary with the background electrolyte containing phosphate. During preconditioning, nebulizer gas was turned off to avoid contamination of MS detector with phosphate ions. To detect nucleotides using the CE positive mode at a pH 7.5, it was necessary to apply air pressure to the inlet capillary during electrophoresis to supplement the electroosmotic flow (EOF) toward the cathode. Moreover, we exchanged the running electrolyte every analysis using the buffer replenishment system to obtain the required reproducibility. Under the optimized conditions, 14 phosphorylated species such as nucleotides, nicotinamide–adenine dinucleotides and coenzyme A (CoA) compounds were well determined in less than 20 min. The relative standard deviations ( $n=6$ ) of the method were better than 0.9% for migration times and between 1.7% and 8.1% for peak areas. The detection limits for these species were between 0.5 and 1.7  $\mu\text{mol/L}$  with pressure injection of 50 mbar for 30 s (30 nL) at a signal-to-noise ratio of 3. This approach is robust and quantitative compared to the previous method, and its utility is demonstrated by the analysis of intracellular nucleotides and CoA compounds extracted from *Escherichia coli* wild type, *pfkA* and *pfkB* knockout mutants. The methodology was used to suggest that *pfkA* is the main functional enzyme.

© 2007 Elsevier B.V. All rights reserved.

**Keywords:** Nucleotide; CoA; Metabolomics; CE–MS; LC–MS/MS; Phosphate; Silanol mask; *Escherichia coli*; Enzyme activity

## 1. Introduction

Metabolites are the end products of cellular regulatory processes, and hence the measurement of the level of all intracellular metabolites can become a new tool for gaining insight into functional genomics. However, unlike other functional genomic approaches, development of metabolome analysis has been largely neglected. As the importance of metabolome analysis is recognized, several large-scale metabolite analysis methods using GC–MS [1,2], LC–MS [3], NMR [4–6], or Fourier transform ion cyclotron resonance mass spectrometry (FT-ICRMS) [7,8] have been developed.

Recently, CE–MS has emerged as a powerful new tool for the analysis of charged species [9–14]. In this marriage

of techniques, CE confers rapid analysis and efficient resolution, and MS provides excellent selectivity and sensitivity. The major advantages of CE–MS are that this methodology exhibits extremely high resolution for even isomers and that virtually any charged species can be infused into MS and directly determined. Previous work in our laboratory demonstrated that CE–MS techniques were quite useful for the metabolome analysis (e.g., 1692 intracellular metabolites from *Bacillus subtilis* extract were simultaneously determined, which revealed the TCA cycle were activated during *B. subtilis* sporulation [15], changes in 88 key metabolites of central metabolism of rice leaves in the daytime and nighttime were successfully quantified [16], and more recently a new biomarker that indicates acetaminophen-induced acute hepatitis has been discovered by differential metabolomics using CE–TOFMS [17]).

In CE, all cations migrate toward the cathode based on their charge and size, whereas all anions move to the opposite direction. Therefore, theoretically all charged species could be determined using two CE–MS configurations. However, there

\* Corresponding author at: Institute for Advanced Biosciences, Keio University, Tsuruoka, Yamagata 997-0052, Japan. Tel.: +81 235 29 0528; fax: +81 235 29 0574.

E-mail address: [soga@sfc.keio.ac.jp](mailto:soga@sfc.keio.ac.jp) (T. Soga).



was one major difficulty that several anions such as nucleotides and CoA compounds adsorbed on the cationic-coated capillary that enabled successful anion analysis in CE–MS [18]. Cao and Moini [19] developed a pressure-assisted CE–MS (PACE–MS) method to the analysis of peptides, and the authors applied the similar a PACE–MS method using a non-charged polymer coated capillary to prevent sample adsorption [18]. Although the method enabled the simultaneous determination of nucleotides and CoA compounds, recently we have found that this approach was not ideal. Notably, the current often fluctuated during electrophoresis, caused migrating time shift of analytes. Additionally, the capillary inlet frequently clogged.

Here, we propose a new PACE–MS method for the analysis of nucleotides and CoAs using a normal fused-silica capillary where silanols are masked with phosphates to prevent nucleotides from interacting with the capillary wall. Nucleotides were driven toward the cathode by both EOF [20] and applied air pressure, followed by MS detection. This approach is reproducible, quantitative and robust and it was readily applied to the simultaneous analysis of nucleotides from *E. coli* samples.

## 2. Experimental

### 2.1. Chemicals

ADP, GDP, CTP, CDP, CMP and succinyl CoA were purchased from Sigma (St. Louis, MO), and 2-morpholinoethanesulfonate (MES, internal standard) from Dojindo (Kumamoto, Japan). All other reagents were obtained from Wako (Osaka, Japan). Individual stock solutions at a concentration of 10 mM were prepared in Milli-Q water, except for AMP in 0.1 M NaOH. The working mixture standard was prepared by diluting these stock solutions with Milli-Q water just before injection. Ammonium acetate electrolyte solution was prepared with ammonium acetate and acetic acid. Ammonium borate solution was with aqueous ammonium and boric acid, and ammonium phosphate was with aqueous ammonium and potassium dihydrogen phosphate. The pH of all solutions was adjusted with aqueous ammonium. The chemicals used were of analytical or reagent grade. Water was purified with a Milli-Q purification system (Millipore, Bedford, MA).

### 2.2. Bacterial strains and growth conditions

*E. coli* BW25113 [*lacI*<sup>H</sup> *rrnB*<sub>T14</sub>  $\Delta$ *lacZ*<sub>WJ16</sub> *hsdR514*  $\Delta$ *araBAD*<sub>AH33</sub>  $\Delta$ *rhaBAD*<sub>LD78</sub>] and its *pfkA* (JWK 3887) and *pfkB* (JWK 5280) knockout mutants [21], were used for this study. The minimal medium was used and it contained 48 mM Na<sub>2</sub>HPO<sub>4</sub>, 22 mM KH<sub>2</sub>HPO<sub>4</sub>, 10 mM NaCl and 45 mM (NH<sub>4</sub>)<sub>2</sub>SO<sub>4</sub>. The following components were sterilized separately and then added (per liter of final medium): 1 mL of 1 M MgSO<sub>4</sub>, 1 mL of 1 mg of vitamin B1/L (filter sterilized) and 10 mL of trace element solution containing (per liter) 0.56 g of CaCl<sub>2</sub>, 0.8 g of FeCl<sub>3</sub>, 0.1 g of MnCl<sub>2</sub>·4H<sub>2</sub>O, 0.17 g of ZnCl<sub>2</sub>, 0.043 g of CuCl<sub>2</sub>·2H<sub>2</sub>O, 0.06 g of CoCl<sub>2</sub>·6H<sub>2</sub>O and 0.06 g Na<sub>2</sub>MoO<sub>4</sub>·2H<sub>2</sub>O. Batch and chemostat cultivations were performed with 4 g/L of glucose and cultures were conducted at

37 °C in a 2 L reactor (BMJ-02 PI, ABLE Co., JAPAN) with pH controlled at 7.0 [22]. The dilution rate for chemostat culture was 0.2/h. Growth was monitored by measuring optical density (OD) at 600 nm, and cells were collected at steady state.

### 2.3. Metabolite extraction

The metabolite extraction procedure from *E. coli* was employed by modifying a previously described procedure [13]. An equal number of cells in culture medium were obtained for every sample based on the OD (20 OD mL) and was passed through a 0.45  $\mu$ m pore size filter. Residual *E. coli* cells on the filter were washed with Milli-Q water and then plunged into 5 mL of methanol, containing internal standards (2  $\mu$ M each trimesate and MES), to inactivate enzymes. After a 10 min incubation at room temperature, 4 mL of the methanol solution was obtained and 4 mL of chloroform and 1.6 mL of Milli-Q water were added to the solution. The mixture was thoroughly mixed with centrifugal filtration at 2300  $\times$  g for 5 min to remove phospholipids liberated from cell membranes. The separated 4 mL methanol–water layer was centrifugally filtered through a Millipore 5-kDa-cutoff filter to remove proteins. The filtrate was lyophilized and dissolved in 50  $\mu$ L of Milli-Q water before PACE–MS analysis.

### 2.4. Instrumentation

All CE–ESI–MS experiments were performed using an Agilent CE Capillary Electrophoresis System equipped with air pressure pump, an Agilent 1100 series MSD quadrupole mass spectrometer, an Agilent 1100 series isocratic HPLC pump, a G1603A Agilent CE–MS adapter kit and a G1607A Agilent CE–ESI–MS sprayer kit (all Agilent Technologies, Waldbronn, Germany). All system control, data acquisition and MSD data evaluation were performed via a G2201A Agilent ChemStation software for CE–MSD.

LC–MS/MS experiments were performed using an Agilent 1100 series HPLC system and an API 3000 triple-quadrupole tandem mass spectrometer (Applied Biosystems, Foster City, CA, USA), and data evaluation were done with the Applied Biosystems Analyst software.

### 2.5. CE–MS conditions

Separations were carried out on a fused-silica capillary with 50  $\mu$ m i.d.  $\times$  100 cm total length. The electrolyte for the CE separation was 50 mM ammonium acetate solution, pH 7.5. Prior to first use, a new capillary was pretreated for 20 min with preconditioning buffer, 25 mM ammonium acetate–75 mM sodium phosphate solution, pH 7.5. Before each injection, the capillary was equilibrated for 10 min by flushing with the preconditioning buffer and subsequently for 6 min with the running electrolyte, which was replenished every run using a buffer replenishment system equipped with the Agilent CE. Sample was injected with a pressure injection of 50 mbar for 30 s (approximately 30 nL). The applied voltage was set at 30 kV and a pressure of 50 mbar was added to the inlet capillary during run. The capillary tem-



perature was thermostatted to 20 °C and the sample tray was cooled below 5 °C. The Agilent 1100 series pump equipped with 1:100 splitter was used to deliver 10 µL/min of 5 mM ammonium acetate in 50% (v/v) methanol–water to the CE interface where it is used as a sheath liquid around the outside of the CE capillary to provide a stable electrical connection between the tip of the capillary and grounded electrospray needle.

ESI–MS was conducted in the negative ion mode and the capillary voltage was set at 3500 V. The nebulizing gas, heated dry nitrogen gas (heater temperature 300 °C), was switched off during the preconditioning step, and a pressure of 10 psi was applied 0.1 min after sample injection using the CE system's timetable. Since the nebulizing gas caused sample aspiration into the capillary inlet, switching it off during sample injection was necessary to enable reliable quantitative analysis. Monovalent deprotonated  $[M - H]^-$  ions for nucleotides and nicotinamide-adenine dinucleotides and divalent deprotonated  $[M - 2H]^{2-}$  ions for CoA compounds were monitored using selective ion monitoring mode.

### 2.6. LC–MS/MS Conditions

The column used was an Asahipak ODP-50 2D (2.0 mm i.d. × 15 cm), (Shodex, Tokyo, Japan). The mobile phase was 5 mM ammonium acetate aqueous solution at a flow-rate of 0.2 mL/min. The temperature of the column oven was 20 °C and the sample injection volume was 1 µL.

ESI–MS was conducted in the negative ion mode and the capillary voltage was set at 4000 V. Nebulizer gas, air curtain gas, nitrogen turbo gas temperature and ionspray voltage were set at 15, 15, 400 °C and –4000 V, respectively. MS/MS with multiple reaction monitoring (MRM) detection was performed to obtain sufficient selectivity and sensitivity.

## 3. Results and discussion

### 3.1. Prevention of nucleotide adsorption by masking silanols with phosphates

The choice of the background electrolyte and pH is most important in developing a CE–MS method. Oppenheimer [23] reported that the chemical stability of nicotinamide adenine dinucleotides (NAD<sup>+</sup>/NADH) depends on the pH conditions. The reduced nicotinamide adenine dinucleotide (NADH) is extremely labile in acidic condition, while its oxidized form (NAD<sup>+</sup>) is readily decomposed in dilute base solution [23,24]. Similarly, flavin adenine dinucleotide (FAD) is decomposed in alkaline solution; on the contrary, CoA is stable at high pH condition. Fortuitously, both nicotinamide adenine dinucleotides and other compounds are stable in a narrow range of pH centered around physiological conditions [23]. Therefore, pH of 7.5 was selected for all the subsequent experiments.

Initially, the influence of background electrolyte on the separation of nucleotides was investigated using a fused-silica capillary and CE with diode array detection. Fig. 1 shows the results of the electropherograms of AMP, ADP and ATP obtained by using 50 mM each of ammonium acetate, ammonium borate

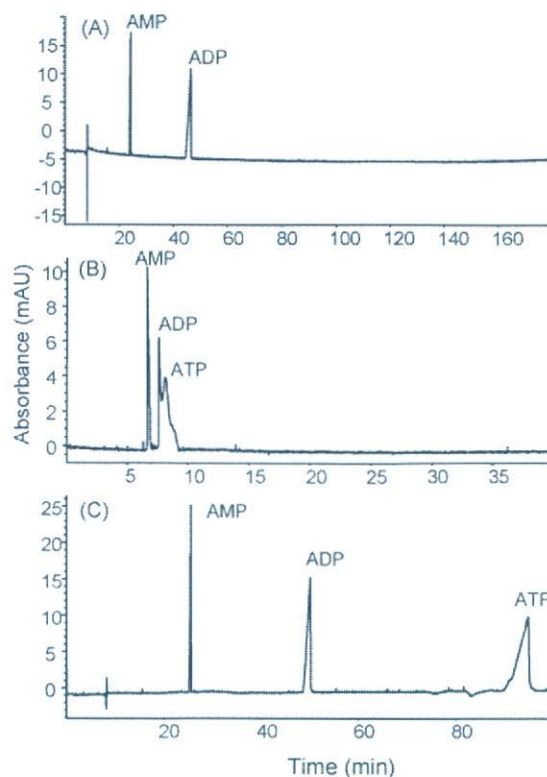


Fig. 1. Comparison of 1 mM each AMP, ADP and ATP detection in CE obtained with (A) ammonium acetate, (B) ammonium borate and (C) ammonium phosphate electrolyte. Experimental conditions: capillary, fused-silica 50 µm i.d. × 80.5 cm (effective length 72 cm); electrolyte, 50 mM, pH 7.5 each; applied potential, 30 kV; injection, 4 s at 50 mbar; temperature, 20 °C; detection, 200 nm.

and ammonium phosphate electrolyte at pH 7.5, respectively. When using ammonium acetate, which is a volatile buffer and commonly used for CE–MS and LC–MS, ATP was not detected within 180 min (Fig. 1A). The peak shapes of ADP and ATP were deteriorated with borate electrolyte (Fig. 1B). However, phosphate electrolyte provided a well-defined ADP and ATP peaks as well as AMP (Fig. 1C). We analyzed them three times by replacing new capillary, electrolyte and standards, and obtained the reproducible results. The equivalent phenomena were observed even when sodium borate and sodium phosphate electrolytes were used. Moreover, we analyzed GMP, GDP and GTP using ammonium acetate electrolyte and obtained considerably broadened GDP and GTP peaks. However, ammonium phosphate electrolyte, pH 7.5 provided defined peak shape of GDP and GTP. Several papers report that silanol groups show adsorptive interaction with phosphate groups based on hydrogen bonding [25,26]. Since silanol groups on bare silica are supposed to have a  $pK_a$  of 7.1 [27,28], the undissociated silanols are approximately 29% at pH 7.5, as estimated based on the Henderson–Hasselbalch equation [29,30]:

$$q = -1/(1 + 10^{pH - pK_a})$$

where  $q$  is the net charge.

We, therefore, assumed that multi-phosphorylated compounds such as ADP, ATP, GDP and GTP might adsorptively interact with undissociated silanols on the fused-silica capil-



lary. Hence, these multi-phosphorylated nucleotides were not detected or showed broadened peaks except when phosphate electrolyte was employed possibly since it was preferentially adsorbed on and masked silanols [25], which realized successful separation and detection of all nucleotides.

While separation was improved, non-volatility of phosphate electrolyte significantly reduced MS detection sensitivity. As Kim et al. [28] used phosphoric acid to block silanol groups on the silica capillary column in LC–MS analysis, we have developed a strategy that masks silanols by preconditioning with electrolyte containing phosphate ions, then subsequently analyzing nucleotides with CE–MS using phosphate-free volatile electrolyte. In this investigation, 25 mM ammonium acetate electrolytes (pH 7.5) containing three different concentrations of phosphate, i.e., 50, 75 and 100 mM, respectively, were used as the preconditioning buffer. The capillary was preconditioned using these buffers for 10 min, followed by running electrolyte (50 mM ammonium acetate, pH 7.5) for 6 min prior to sample analysis. Although slight decrease in peak areas of ATP, NAD and NADH were observed, every nucleotide exhibited better reproducibility when using 25 mM ammonium acetate (pH 7.5) containing 75 mM phosphate.

After masking silanols on the capillary with the above-mentioned preconditioning buffer followed by washing the capillary with the 50 mM ammonium acetate (pH 7.5) running electrolyte, nucleotides were separated by CE positive mode and detected by MS negative ion mode. While the nucleotides themselves migrated towards the anode (opposite the MS direction), they were driven to the cathode by electroosmotic flow (EOF) at the pH 7.5. It was also necessary to maintain constant liquid flow toward the MS by applying air pressure to the inlet capillary during electrophoresis in order to reduce analysis time (Fig. 2). This PACE–MS approach provided good resolution of every analyte, however, considerable fluctuations in migration time of all nucleotides were observed (Fig. 3A). We found that the fluctuations in migration time were caused by the decrease in the pH of the running electrolyte from 7.5 to 5.8 in eight runs. This was due to little or no buffering capacity of ammonium acetate at pH 7.5. To resolve the problem, we replenished the running electrolyte every analysis using the CE instrument's buffer replenishment system to maintain a constant pH of 7.5 of the electrolyte. This technique dramatically improved migration time fluctuation of every peak (Fig. 3B).

It was found that turning off nebulizer nitrogen gas, used to assist electrospray ionization, between runs resulted in better reproducibilities of peak areas for all nucleotides. It is assumed that stopping electrospray during preconditioning the capillary prevents contamination of the MS detector with phosphate ions contained in the preconditioning buffer.

### 3.2. Method validation

Fig. 4 shows selected ion electropherograms of the 14-nucleotide standard mixture including nicotinamide–adenine dinucleotides and acetyl CoA obtained by the optimized PACE–MS method. Although most of compounds were successfully detected as their monovalent deprotonated molecular

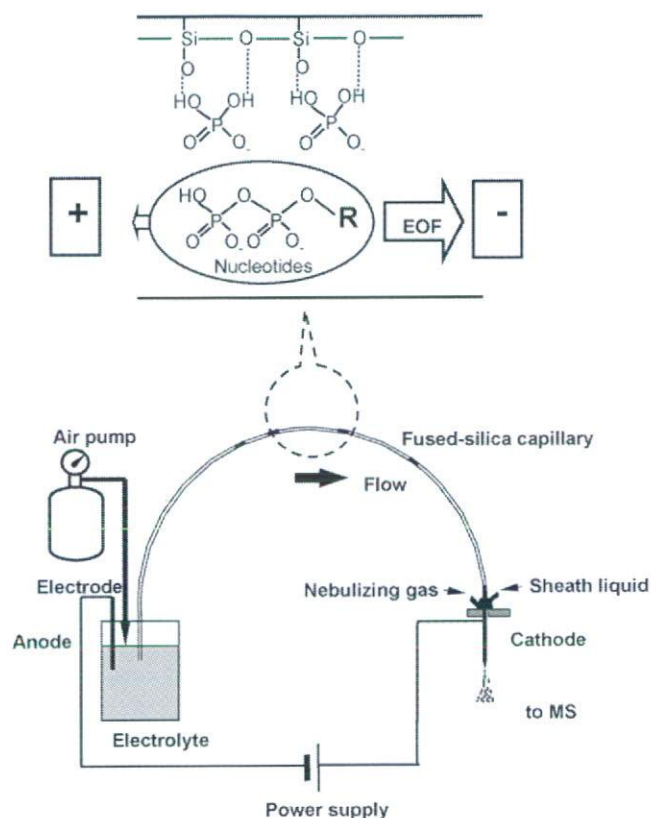


Fig. 2. Schematic of nucleotide analysis by the PACE–MS system. As shown in zoom-in-view, silanols are masked by phosphate ions prior to sample injection to prevent multi-phosphorylated species from adsorptively interacting with the fused-silica capillary. While nucleotides migrate toward the anode, they are driven to the cathode by both EOF and application of air pressure to the inlet capillary and analyzed by the MS detector.

$[M - H]^-$  ions, intensity in divalent  $[M - 2H]^{2-}$  ion of acetyl CoA was higher than that in monovalent ion. The reproducibility, linearity and sensitivity of the method were investigated and data obtained by using the optimized conditions are listed in Table 1. Good reproducibility was obtained for both migration times and peak areas, as indicated in the table. The calibration curves for all species were between 0.997 and 0.999 at 10, 20, 50, 100, 200 and 500  $\mu\text{mol/L}$  with correlation coefficients. The concentration detection limits for all components were better than 1.7  $\mu\text{mol/L}$  with pressure injection of 50 mbar for 30 s (30 nL) at a signal-to-noise ratio of 3. These results indicate that the proposed method can be useful for simultaneous and quantitative analysis of nucleotides, nicotinamide–adenine dinucleotides and CoA compounds.

### 3.3. Analysis of nucleotides of *E. coli*

While nucleotides are well known as the building blocks of DNA and RNA, they are involved in almost all the activities of cells. Some nucleotides such as ATP, NAD, NADH function as co-substrates, and others such as cyclic AMP are regulatory compounds. The utility of the proposed PACE–MS method was demonstrated by the simultaneous analysis of nucleotides, nicotinamide–adenine dinucleotides, and

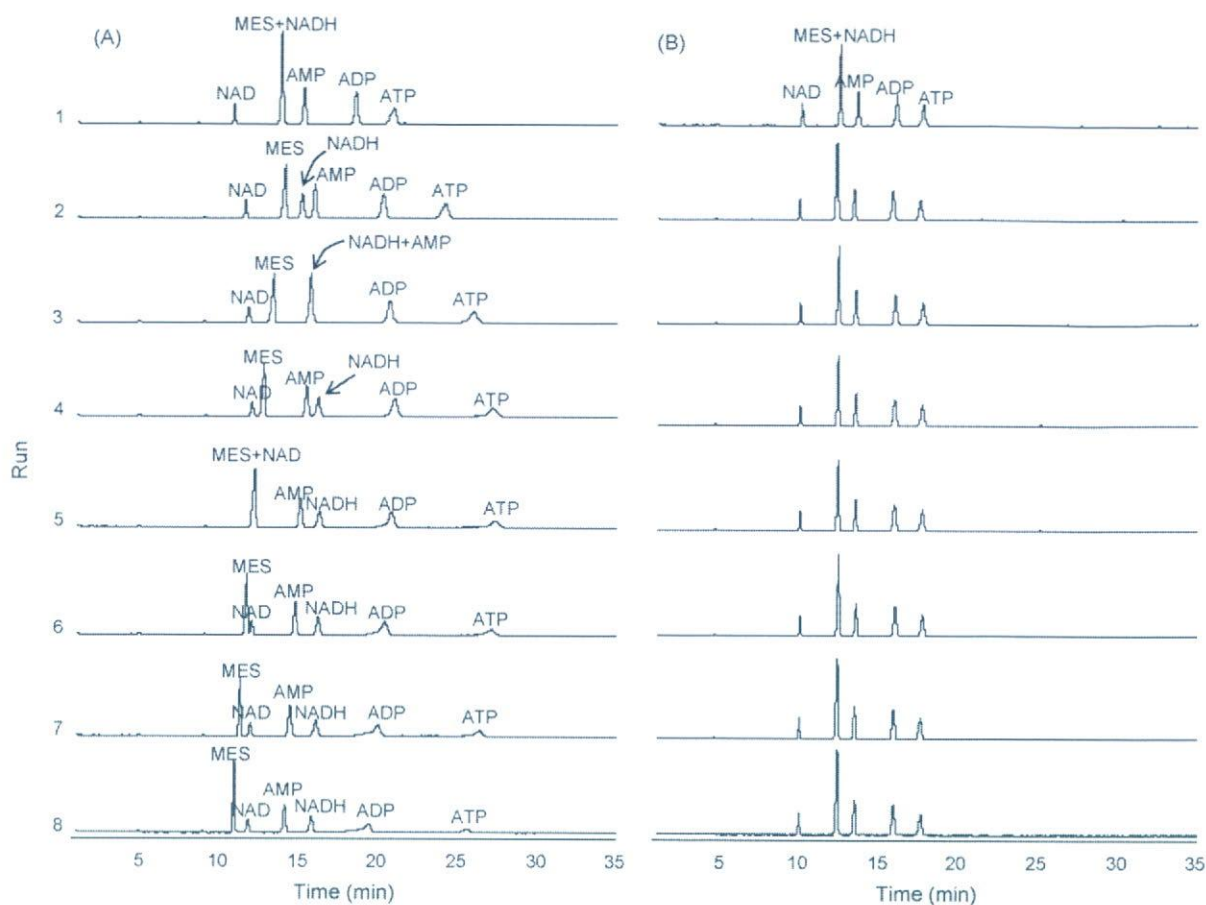


Fig. 3. Effect of buffer replenishment on reproducibility of nucleotide migration time. Nucleotide standard mixture (100  $\mu$ M each) containing MES (internal standard) were analyzed with (A) the same electrolyte and (B) the buffer replenished every run. Experimental conditions: capillary, fused-silica 50  $\mu$ m i.d.  $\times$  100 cm; preconditioning, 25 mM ammonium acetate (pH 7.5) containing 75 mM phosphate for 10 min followed by 50 mM ammonium acetate electrolyte (pH 7.5) for 6 min; applied potential, 30 kV; applied pressure, 50 mbar; sample injection, 30 s at 50 mbar (30 nL); temperature, 20  $^{\circ}$ C; sheath liquid, 10  $\mu$ L/min of 5 mM ammonium acetate in 50% (v/v) methanol-water; MS detector polarity, negative; capillary voltage, 3500 V; fragmentor voltage, 100 V; drying gas,  $N_2$ ; drying gas temperature, 300  $^{\circ}$ C; nebulizer gas pressure, 10 psig.

flavin adenine dinucleotides, and CoA compounds in *E. coli* extracts.

Fig. 5A shows the results for the analysis of nucleotides and CoA related compounds extracted from *E. coli* BW25113

(wild type) cells ( $OD_{600\text{ nm}} = 4.38$ ). CoA compounds such as CoA, acetyl CoA and succinyl CoA were detected at their divalent deprotonated ions. The peaks were identified by comparing their molecular weights and migration times with those

Table 1  
Reproducibility, linearity and sensitivity

	RSD ( $n=6$ ) (%)			Detection limit
	Migration time	Peak area	Linearity correlation	Concentration ( $\mu$ M)
CMP	0.4	3.2	0.998	1.0
AMP	0.3	2.9	0.997	1.3
GMP	0.4	1.7	0.998	0.6
CDP	0.6	1.9	0.998	1.5
ADP	0.6	3.1	0.999	1.6
GDP	0.6	3.1	0.999	0.7
CTP	0.9	3.3	0.999	1.7
ATP	0.8	4.3	0.999	0.6
GTP	0.7	3.7	0.999	1.4
NAD	0.3	3.7	0.999	0.5
NADP	0.4	6.1	0.998	0.8
NADH	0.3	8.1	0.999	0.9
NADPH	0.7	5.8	0.997	0.9
Acetyl CoA	0.5	2.2	0.999	0.5



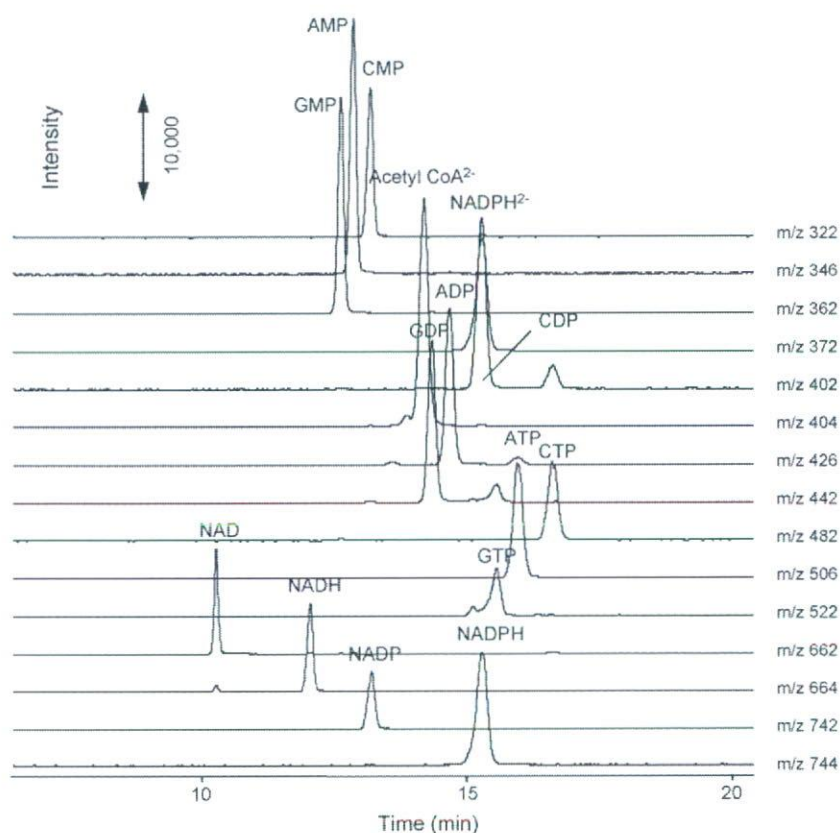


Fig. 4. PACE-MS selected ion electropherograms for standard mixture (100  $\mu$ M each) of nucleotides, nicotinamide-adenine dinucleotides and CoA compounds. Experimental conditions: nebulizer gas pressure, 10 psig after 0.1 min. Other experimental conditions are the same as in Fig. 3.

Table 2  
Nucleotide concentration of *E. coli* BW25113 wild type,  $\Delta$ *pfkA* and  $\Delta$ *pfkB* knockout mutant

Compound	Wild type			$\Delta$ <i>pfkA</i>	$\Delta$ <i>pfkB</i>
	Concentration ( $\mu$ M)	RSD ( $n = 35$ ) (%)	Recovery rate ( $n = 3$ )(%)	Concentration ( $\mu$ M)	Concentration ( $\mu$ M)
TMP	693	2.9	95.7 $\pm$ 4.8	91	38
cAMP	10	19	93.1 $\pm$ 2.5	2	9
cGMP	nd <sup>a</sup>	–	94.5 $\pm$ 3.1	19	nd <sup>a</sup>
AMP	890	2.8	100.0 $\pm$ 5.8	547	1060
GMP	81	4.2	94.5 $\pm$ 4.5	73	99
CoA	30	28	90.4 $\pm$ 1.6	94	66
TDP	1260	4.0	95.8 $\pm$ 3.1	728	64
CDP	338	3.6	97.7 $\pm$ 3.4	256	179
Acetyl CoA	358	2.5	93.8 $\pm$ 4.2	74	127
ADP	1427	5.0	94.3 $\pm$ 4.8	340	670
Succinyl CoA	nd <sup>a</sup>	–	95.6 $\pm$ 2.9	6	nd
GDP	439	5.1	95.8 $\pm$ 5.1	146	248
TTP	148	5.7	93.2 $\pm$ 6.0	28	133
CTP	324	4.6	92.9 $\pm$ 5.1	111	320
ATP	1640	5.7	97.6 $\pm$ 3.8	239	1560
GTP	696	4.9	92.0 $\pm$ 5.2	95	680
NAD	1200	2.9	101.7 $\pm$ 2.7	391	941
NADH	nd <sup>a</sup>	–	83.7 $\pm$ 4.5	nd <sup>a</sup>	nd <sup>a</sup>
NADP	209	5.1	92.2 $\pm$ 2.1	39	162
NADPH	nd <sup>a</sup>	–	70.1 $\pm$ 5.3	nd <sup>a</sup>	nd <sup>a</sup>
FAD	16	8.6	95.4 $\pm$ 4.5	8	55

<sup>a</sup> nd; not detected.

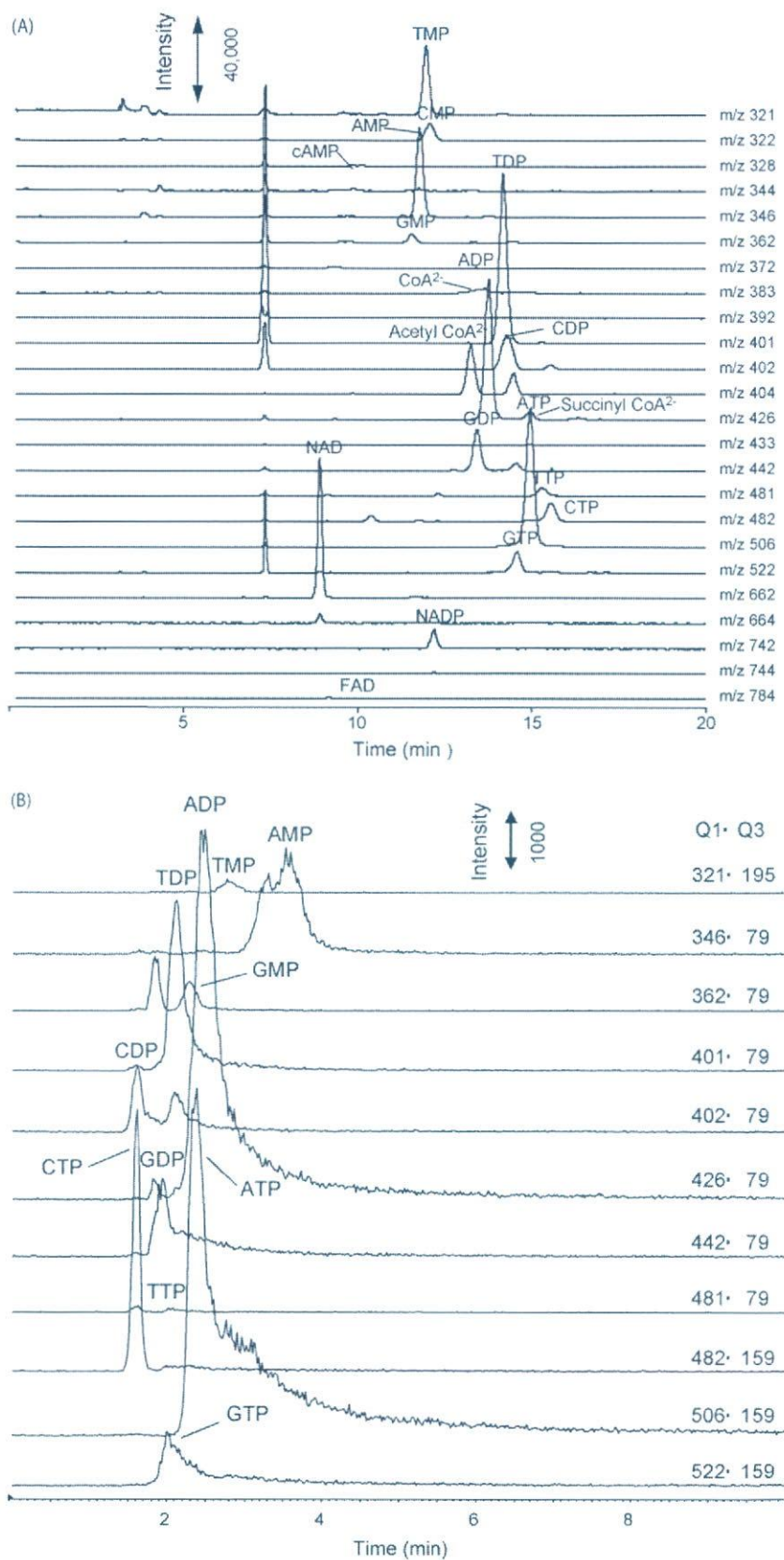


Fig. 5. Comparison of (A) PACE-MS and (B) LC-MS/MS analysis of nucleotides, nicotinamide-adenine dinucleotides and CoA compounds in the extract from *E. coli* BW25113 wild type. Experimental conditions of PACE-MS: the same as in Fig. 4. For conditions of LC-MS/MS, see Section 2. The optimized parameters, Q1 (precursor ion), Q3 (product ion), declustering potential, focusing potential, collision energy and collision cell exit potential are listed in Table 3.



Table 3  
Optimized MRM parameters for each nucleotide in LC–MS/MS

Nucleotide	Q1 ( <i>m/z</i> )	Q3 ( <i>m/z</i> )	Declustering potential (V)	Focusing potential (V)	Collision energy (V)	Collision cell exit potential (V)
TMP	321	195	–52	–82	–22	–6
AMP	346	79	–58	–103	–52	–4
GMP	362	79	–45	–90	–38	–5
TDP	401	79	–48	–86	–59	–5
CDP	402	79	–50	–170	–58	–3
ADP	426	79	–41	–90	–60	–5
GDP	442	79	–50	–100	–68	–5
TTP	481	159	–46	–100	–40	–9
CTP	482	159	–58	–160	–34	–6
ATP	506	159	–41	–104	–42	–7
GTP	522	159	–54	–177	–45	–8

of nucleotide and CoA standards and were quantified (Table 2). The relative standard deviations ( $n = 35$ ) for the amounts of identified compounds in the sample were better than 6% except for small compounds. Under these conditions, however, neither NADH nor reduced nicotinamide–adenine dinucleotide phosphate (NADPH) could be observed. To investigate quantification accuracy and ion suppression effect in this system, we analyzed cell extracts of wild type *E. coli* BW25113 spiked with 100  $\mu$ M of each standard and calculated the recovery (Table 2) and compared with the results obtained by the LC–MS/MS method (Fig. 5B). Except for nicotinamide–adenine dinucleotide derivatives (NADPH/NADP<sup>+</sup>), the recovery rates of metabolites in the PACE–MS were higher than 90%. Surprisingly, the recovery rates in LC–MS/MS were quite low. Those of TMP, AMP, GMP, TDP, CDP, ADP, GDP, TTP, CTP, ATP and GTP in LC–MS/MS were 62, 25, 40, 43, 25, 31, 27, 21, 37, 23 and 19%, respectively. Considering the good linearity of calibration curves in the concentration ranges of the LC–MS/MS method, these poor recovery rates may be caused by ion suppression effect because all nucleotides were retained poorly (Fig. 5B) and eluted together with other charged components in *E. coli* extracts. On the other hand, the PACE–MS provides much better resolution for nucleotides compared to LC–MS/MS. In addition, the injection volume in the PACE–MS (30 nL) is considerably small compared to that in LC–MS/MS (1  $\mu$ L). Therefore, the PACE–MS seems to be scarcely affected by ion suppression effect and it enables sufficient quantitative analysis for most nucleotides and CoA compounds. As the conversion of NADH to NAD or NADPH to NADP occurs depending on physical conditions such as sample pH and temperature, further examination for sample treatment is required to quantify them correctly (Table 3).

We also analyzed nucleotide and CoA related compounds in the knockout mutant of *E. coli* BW25113 *pfkA* or *pfkB*, the isoenzyme that catalyzes the production of fructose 1,6-bisphosphate from fructose 6-phosphate in glycolytic pathway. The results were compared with *E. coli* BW25113 wild type (Table 2) and distinct amount differences in many compounds between samples were observed. It was found that considerable decrease in the acetyl CoA, ADP, ATP, NAD, NADH and FAD levels in the *pfkA* mutant compared to those in the *pfkB* mutant, which may suggest that deletion of *pfkA* had significant effect of metabolism

of glycolytic and the TCA pathway. This hypothesis that *pfkA* can be the dominant enzyme in *E. coli*, is supported by a previous study [31].

#### 4. Conclusions

A new pressure-assisted CE–MS method for the analysis of nucleotides has been developed. Compared with other techniques, this method has several advantages: (1) various types of phosphorylated species such as nucleotides, nicotinamide–adenine dinucleotides and CoA compounds are simultaneously analyzed; (2) sensitivity and selectivity are sufficient for quantification; and (3) good reproducibility, linearity and robustness are obtained. Its utility was demonstrated by the analysis of these phosphorylated species in *E. coli* wild type, *pfkA* or *pfkB* knockout mutant and the results can potentially provide valuable information about the enzyme activity. The PACE–MS method developed in this study can be a promising new tool for the analysis of nucleotides, nicotinamide–adenine dinucleotides and CoA compounds in biological samples.

#### Acknowledgments

We thank Dr. Kenji Nakahigasi, Dr. Takashi Hirasawa, Miki Naba and Kenta Hirai, Institute for Advanced Biosciences, Keio University, for technical support and Dr. David N. Heiger, Agilent Technologies, for critical reading of the manuscript. This work was supported in part by a grant the 21st Century COE Program entitled “Understanding and Control of Life’s Function via Systems Biology” and a grant-in-aid for scientific research on priority areas “Lifesurveyor” from the Ministry of Education, Culture, Sport, Science and Technology (MEXT) of Japan as well as research funds from Yamagata prefectural government and Tsuruoka city.

#### References

- [1] O. Fiehn, J. Kopka, P. Dormann, T. Altmann, R.N. Trethewey, L. Willmitzer, *Nat. Biotechnol.* 18 (2000) 1157.
- [2] N. Schauer, Y. Semel, U. Roessner, A. Gur, I. Balbo, F. Carrari, T. Pleban, A. Perez-Melis, C. Bruedigam, J. Kopka, L. Willmitzer, D. Zamir, A.R. Fernie, *Nat. Biotechnol.* 24 (2006) 447.



- [3] R. Plumb, J. Granger, C. Stumpf, I.D. Wilson, J.A. Evans, E.M. Lenz, *Analyst* 128 (2003) 819.
- [4] N.V. Reo, *Drug Chem. Toxicol.* 25 (2002) 375.
- [5] M. Coen, E.M. Lenz, J.K. Nicholson, I.D. Wilson, F. Pognan, J.C. Lindon, *Chem. Res. Toxicol.* 16 (2003) 295.
- [6] M. Coen, S.U. Ruepp, J.C. Lindon, J.K. Nicholson, F. Pognan, E.M. Lenz, I.D. Wilson, *J. Pharm. Biomed. Anal.* 35 (2004) 93.
- [7] A. Aharoni, C.H. Ric de Vos, H.A. Verhoeven, C.A. Maliepaard, G. Kruppa, R. Bino, D.B. Goodenowe, *Omics* 6 (2002) 217.
- [8] M.Y. Hirai, M. Yano, D.B. Goodenowe, S. Kanaya, T. Kimura, M. Awazuhara, M. Arita, T. Fujiwara, K. Saito, *Proc. Natl. Acad. Sci. USA* 101 (2004) 10205.
- [9] S.K. Johnson, L.L. Houk, D.C. Johnson, R.S. Houk, *Anal. Chim. Acta* 389 (1999) 1.
- [10] W. Lu, G.K. Poon, P.L. Carmichael, R.B. Cole, *Anal. Chem.* 68 (1996) 668.
- [11] M. Moini, *Methods Mol. Biol.* 276 (2004) 253.
- [12] T. Soga, D.N. Heiger, *Anal. Chem.* 72 (2000) 1236.
- [13] T. Soga, Y. Ueno, H. Naraoka, Y. Ohashi, M. Tomita, T. Nishioka, *Anal. Chem.* 74 (2002) 2233.
- [14] C.C. Liu, J.S. Huang, D.L. Tyrrell, N.J. Dovichi, *Electrophoresis* 26 (2005) 1424.
- [15] T. Soga, Y. Ohashi, Y. Ueno, H. Naraoka, M. Tomita, T. Nishioka, *J. Proteome Res.* 2 (2003) 488.
- [16] S. Sato, T. Soga, T. Nishioka, M. Tomita, *Plant J.* 40 (2004) 151.
- [17] T. Soga, R. Baran, M. Suematsu, Y. Ueno, S. Ikeda, T. Sakurakawa, Y. Kakazu, T. Ishikawa, M. Robert, T. Nishioka, M. Tomita, *J. Biol. Chem.* 281 (2006) 16768.
- [18] T. Soga, Y. Ueno, H. Naraoka, K. Matsuda, M. Tomita, T. Nishioka, *Anal. Chem.* 74 (2002) 6224.
- [19] P. Cao, M. Moini, *Electrophoresis* 19 (1998) 2200.
- [20] K.D. Lukacs, J.W. Jorgenson, *J. High Res. Chromatogr.* 8 (1985) 407.
- [21] T. Baba, T. Ara, M. Hasegawa, Y. Takai, Y. Okumura, M. Baba, K.A. Datsenko, M. Tomita, B.L. Wanner, H. Mori, *Mol. Syst. Biol.* (2006), doi:10.1038/msb4100050.
- [22] J. Zhao, T. Baba, H. Mori, K. Shimizu, *Metab. Eng.* 6 (2004) 164.
- [23] N.J. Oppenheimer, in: D. Dolphin, R. Poulson, O. Avramovic (Eds.), *Pyridine Nucleotide Coenzymes Part B (Coenzymes and Cofactors)*, 2, John Wiley & Sons, New York, NY, 1987, p. 323.
- [24] N.O. Kaplan, S.P. Colowick, C.C. Barnes, *J. Biol. Chem.* 191 (1951) 461.
- [25] Q. Liu, F. Lin, R.A. Hartwick, *Chromatographia* 47 (1998) 219.
- [26] G. Liu, *Chromatographia* 28 (1989) 493.
- [27] M.L. Hair, W. Hertl, *J. Phys. Chem.* 74 (1970) 91.
- [28] J. Kim, D.G. Camp II, R.D. Smith, *J. Mass Spectrom.* 39 (2004) 208.
- [29] F. Benavente, E. Balaguer, J. Barbosa, V. Sanz-Nebot, *J. Chromatogr. A* 1117 (2006) 94.
- [30] M. Sugimoto, S. Kikuchi, M. Arita, T. Soga, T. Nishioka, M. Tomita, *Anal. Chem.* 77 (2005) 78.
- [31] J. Babul, *J. Biol. Chem.* 253 (1978) 4350.



---

# **Polymer Entrapment in Polymerized Silicate for Preparing Highly Stable Capillary Coatings for CE and CE-MS**

---

**Maria Rowena N. Monton, Masaru Tomita, Tomoyoshi Soga, and Yasushi Ishihama**

Institute for Advanced Biosciences, Keio University, Tsuruoka, Yamagata 997-0017, Japan, and PRESTO, Japan Science and Technology Agency, Sanbancho Building, 5-Sanbancho, Chiyodaku, Tokyo 102-0075, Japan

**ANALYTICAL<sup>®</sup>**  
**CHEMISTRY**

Reprinted from  
Volume 79, Number 20, Pages 7838–7844



# Polymer Entrapment in Polymerized Silicate for Preparing Highly Stable Capillary Coatings for CE and CE–MS

Maria Rowena N. Monton,<sup>†</sup> Masaru Tomita,<sup>†</sup> Tomoyoshi Soga,<sup>\*,†</sup> and Yasushi Ishihama<sup>\*,†,‡</sup>

Institute for Advanced Biosciences, Keio University, Tsuruoka, Yamagata 997-0017, Japan, and PRESTO, Japan Science and Technology Agency, Sanbancho Building, 5-Sanbancho, Chiyodaku, Tokyo 102-0075, Japan

An easy-to-implement capillary coating strategy based on polymer entrapment in the network of polymerized silicate is described. In this manner, cationic polymers are tightly fixed onto the inner wall of the capillary for electroosmotic flow control without necessitating complex surface modification chemistries. The resulting coated capillary exhibited good stability over a wide range of pH, good reproducibility, strong endurance in more than 300 electrophoretic runs, and tolerance of commonly employed organic solvent additives in CE. Applications in CE–MS analysis of biologically important anions as well as sample enrichment are shown. Additionally, it was used as a durable base for attachment of multiple layers of charged polymers on the wall, via electrostatic interaction with the preceding layer. Thus, two novel types of highly stable coated capillaries, one with anodic EOF and the other cathodic, were developed.

Capillary electrophoresis (CE) has always been touted as a high-efficiency separation technique, but its potential is seldom fully realized because analyte–wall interactions, compounded by high surface area-to-volume ratios of narrow-bore capillaries, result in some band broadening. Moreover, migration time shifts pose a major problem in CE systems, which rely on matching peak migration times against those of pure standards for identification. The intrinsic electrophoretic mobility of an analyte is constant under a given set of conditions, but its apparent mobility is often less reproducible because of run-to-run variations in electroosmotic flow (EOF).<sup>1</sup> The EOF is a consequence of electroneutrality constraint on the wall. Depending on the separation problem, its direction may be reversed, or its magnitude augmented or diminished, or it may be completely eliminated. Thus, it is important to control surface chemistry. Numerous approaches have been explored for regulating wall properties of fused-silica capillaries, including manipulation of pH,<sup>2</sup> ionic strength,<sup>3</sup> and viscosity<sup>4</sup> of background electrolytes, but the most common strategy is to coat the inner wall of the capillary.

Based on the attachment of the coating onto the wall, coatings are broadly categorized as physically adsorbed or covalently attached.<sup>5</sup> Physically adsorbed coatings result from reversible adsorption of charged (e.g., Polybrene (PB),<sup>6,7</sup> polyethyleneimine (PEI),<sup>8</sup> poly(dimethyldiallylammonium chloride),<sup>9</sup> dextran sulfate (DS),<sup>10</sup> polyarginine<sup>11</sup>) or neutral (e.g., poly(ethylene oxide),<sup>12,13</sup> poly(vinyl alcohol),<sup>14</sup> hydroxyethyl cellulose<sup>15</sup>) polymeric or small-molecule (e.g., cetyltrimethylammonium bromide,<sup>16</sup> didodecyltrimethylammonium bromide,<sup>17</sup> 1,2-dilauroyl-*sn*-phosphatidylcholine,<sup>18</sup> triethylenetetramine,<sup>19</sup> trimethylammonio propane sulfonate,<sup>20</sup> 1,2-dioleoyl-3-trimethylammonio propane<sup>21</sup>) additives on the wall via hydrogen bonding or electrostatic interactions. The coating procedures are fairly simple and generally entail only rinsing the capillary with a dilute aqueous solution of the additive. The working lifetimes of coated capillaries can be easily extended by regeneration, i.e., by rinsing out the additive, and then replacing it with a fresh layer of the same. Physically adsorbed coatings can be either dynamic or static.<sup>5</sup> To compensate for the poor stability of dynamic adsorbed coatings, the additive must be incorporated in the running buffer, and in some cases, this can

- (4) Schwer, C.; Kenndler, E. *Anal. Chem.* **1991**, *63*, 1801–1807.
- (5) Doherty, E. A. S.; Meagher, R. J.; Albarghouti, M. N.; Barron, A. E. *Electrophoresis* **2003**, *24*, 34–54.
- (6) Masselter, S. M.; Zemann, A. J. *Anal. Chem.* **1995**, *67*, 1047–1053.
- (7) Li, M. X.; Liu, L.; Wu, J.-T.; Lubman, D. M. *Anal. Chem.* **1997**, *69*, 2451–2456.
- (8) Erim, F. B.; Cifuentes, A.; Poppe, H.; Kraak, J. C. J. *Chromatogr., A* **1995**, *708*, 356–361.
- (9) Wang, Y.; Dubin, P. L. *Anal. Chem.* **1999**, *71*, 3463–3468.
- (10) Katayama, H.; Ishihama, Y.; Asakawa, N. *Anal. Chem.* **1998**, *70*, 2254–2260.
- (11) Chiu, R. W.; Jimenez, J. C.; Monnig, C. A. *Anal. Chim. Acta* **1995**, *307*, 193–201.
- (12) Iki, N.; Yeung, E. S. J. *Chromatogr., A* **1996**, *731*, 273–282.
- (13) Vayaboury, W.; Kirby, D.; Giani, O.; Cottet, H. *Electrophoresis* **2005**, *26*, 2187–2197.
- (14) Gilges, M.; Kleemiss, M. H.; Schomburg, G. *Anal. Chem.* **1994**, *66*, 2038–2046.
- (15) Kleemiss, M. H.; Gilges, M.; Schomburg, G. *Electrophoresis* **1993**, *14*, 515–522.
- (16) Reijenga, J. C.; Aben, G. V. A.; Verheggen, T. P. E. M.; Everaerts, F. M. J. *Chromatogr.* **1983**, *260*, 241–254.
- (17) Melanson, J. E.; Barylka, N. E.; Lucy, C. A. *Anal. Chem.* **2000**, *72*, 4110–4114.
- (18) Barylka, N. E.; Lucy, C. A. *J. Chromatogr., A* **2002**, *956*, 271–277.
- (19) Corradini, D.; Spreacener, L. *Chromatographia* **2003**, *58*, 587–596.
- (20) MacDonald, A. M.; Sheppard, M. A. W.; Lucy, C. A. *Electrophoresis* **2005**, *26*, 4421–4428.
- (21) Bonoli, M.; Varjo, S. J. O.; Wiedmer, S. K.; Riekkola, M.-L. *J. Chromatogr., A* **2006**, *1119*, 163–169.

\* To whom correspondence should be addressed. E-mail: soga@sfc.keio.ac.jp. Tel: +81-235-29-0528. Fax: +81-235-29-0574. E-mail: y-ishi@ttk.keio.ac.jp. Tel: +81-235-29-0571. Fax: +81-235-29-0536.

<sup>†</sup> Keio University.

<sup>‡</sup> PRESTO, Japan Science and Technology Agency.

(1) Chiari, M.; Cretich, M.; Horvath, J. *Electrophoresis* **2000**, *21*, 1521–1526.

(2) Hayes, M. A.; Kheterpal, I.; Ewing, A. *Anal. Chem.* **1993**, *65*, 27–31.

(3) Green, J. S.; Jorgenson, J. W. *J. Chromatogr.* **1989**, *478*, 63–70.



cause unwanted interactions with the analytes or interference with the detection scheme (e.g., mass spectrometry (MS)). In contrast, static adsorbed coatings, including the so-called semipermanent coatings<sup>17,18,21</sup> and those formed from alternating layers of oppositely charged polymers,<sup>10,22,23</sup> are sufficiently stable and therefore do not require the presence of the additive in the running buffer. By covalent bonding, polymers (e.g., polyacrylamide,<sup>24–27</sup> poly(vinylpyrrolidone),<sup>28</sup> poly(ethylene glycol)<sup>29</sup>) and small molecules (e.g., octadecylsilane)<sup>30</sup> can also be fixed to the wall. In most cases, the capillary surface is initially derivatized with bifunctional reagents to provide anchors<sup>5</sup> through which polymers, either polymerized in situ or preformed, and then subsequently cross-linked to increase surface coverage, are attached to the wall. Coated capillaries prepared using covalent bonding generally exhibit longer working lifetimes than those prepared using physical adsorption method, but the complexity and multiplicity of steps required in the preparation of the former often lead to poor coating-to-coating reproducibility.

Soluble silicates of sodium and potassium have a long history of use in a wide range of bonding and coating applications, and when applied as thin films on or between surfaces, they dry to form tough, tightly adhering inorganic coatings or bonds.<sup>31</sup> To date, polymerized silicates have been exploited in a number of applications for separation science, such as for gluing chromatographic beads together for capillary electrochromatography,<sup>32</sup> for preparing monolithic columns for liquid chromatography,<sup>33</sup> and for immobilizing enzymes at the bottom of a 96-well microtiter plate.<sup>34</sup>

In this paper, we describe a novel way of modifying the inner wall of the capillary based on the immobilization of a positively charged polymer by entrapment in a matrix of polymerized silicate. This technique combines the simplicity in terms of preparation of physically adsorbed coatings with the stability generally characteristic of covalently attached ones. The basic properties of the coated capillary are discussed, and some applications are shown.

## EXPERIMENTAL SECTION

**Reagents.** Potassium silicate solution (Kasil 1) was a gift from PQ Corp. (Valley Forge, PA). Tryptic digest of pig serum albumin was from Michrom Bioresources (Auburn, CA). PB, diethylaminoethyl (DEAE)-dextran, PEI, DS, hexamethyldisilazane (HMDS), horse heart myoglobin, trypsin inhibitor,  $\beta$ -lactoglobulin A, dihydroxyacetone phosphate, glycerol 3-phosphate, 2-phosphoglycer-

ate, 2,3-diphosphoglycerate, 6-phosphogluconate, and erythrose 4-phosphate were from Sigma (St. Louis, MO). All other reagents were obtained from Wako (Osaka, Japan). Buffers and standard solutions were prepared using water purified with a Milli-Q system from Millipore (Bedford, MA), or aqueous–alcoholic solutions.

**Instruments.** CE experiments were performed on an Agilent CE system (Waldbronn, Germany) using fused-silica capillaries (50  $\mu\text{m}$  i.d.  $\times$  360  $\mu\text{m}$  o.d.) from Polymicro Technologies (Phoenix, AZ), uncoated or coated in-house. The capillaries were thermostated at 25 °C. Unless specified otherwise, samples were injected by applying a 50-mbar pressure at the inlet vial for 3 s. EOF mobilities were measured using formamide as electrically neutral marker. Using UV detection, absorbance values were monitored at 200 nm. For CE–MS experiments, the CE instrument was coupled to an Agilent 1100 series MSD mass spectrometer, via a sheath liquid-assisted electrospray ionization (ESI) interface. ESI–MS was conducted in the negative ion mode, with the capillary voltage set at 3500 V. A flow of heated dry nitrogen gas was maintained at 10 L/min. The spectrometer was operated in the selected ion monitoring mode. Other conditions are indicated in relevant text or figures.

All capillary cleaning and coating procedures were carried out at room temperature using Terumo disposable syringes (Tokyo, Japan) and a KD Scientific syringe pump (Holliston, MA). pH measurements and adjustments were made using a Horiba F22 pH meter (Kyoto, Japan). The conductivities of buffer solutions (phosphate, pH 2–3, 6–7; acetate, pH 4–5; borate, pH 8–11) used in EOF versus pH experiments were measured and adjusted to be approximately equal using a Horiba ES-51 conductivity meter (Kyoto, Japan).

**Capillary Coating.** The new capillary was flushed successively with 1 M sodium hydroxide and water for 30 min and then purged with a stream of nitrogen gas for 5 min to dry the surface. The 200  $\mu\text{L}$  of potassium silicate solution (Kasil 1), 200  $\mu\text{L}$  of water, 40  $\mu\text{L}$  of formamide, and 80  $\mu\text{L}$  of aqueous cationic polymer solution were mixed thoroughly, and the resulting mixture was pumped into the capillary (10 min for a 50-cm capillary; 20 min for a 120-cm capillary) at room temperature. After 1 h, the excess coating solution was removed by air-flushing, and the coated capillary was allowed to dry overnight. For multilayer coatings, the preceding drying step was omitted; instead, an aqueous solution of the oppositely charged polymer was rinsed into the capillary (10 min for a 50-cm capillary; 20 min for a 120-cm capillary), allowed to stand for 30 min, and the excess was removed and then either left to dry or the next layer was applied. The concentrations of polymers used in the coatings are indicated in relevant text and figures as % w/v.

## RESULTS AND DISCUSSION

**Polymerized Silicate-Entrapped Polymer for Capillary Coating.** The present coating technique based on polymerized silicate can be likened to laying an additional layer of glass on the inner wall of the capillary, except that this glass layer contains polymeric additives to alter the surface charge (Figure 1A). In this work, potassium silicate (Kasil 1) was polymerized via a sol–gel process, using formamide as drying control chemical additive to increase the mechanical strength of the gel,<sup>35</sup> and mixed with

(22) Katayama, H.; Ishihama, Y.; Asakawa, N. *Anal. Chem.* **1998**, *70*, 5272–5277.

(23) Graul, T. W.; Schlenoff, J. B. *Anal. Chem.* **1999**, *71*, 4007–4013.

(24) Hjerten, S. *J. Chromatogr.* **1985**, *347*, 191–198.

(25) Cobb, K. A.; Dolnik, V.; Novotny, M. *Anal. Chem.* **1990**, *62*, 2478–2483.

(26) Cifuentes, A.; Canajales, P.; Diez-Masa, J. C. *J. Chromatogr., A* **1999**, *830*, 423–438.

(27) Liu, S.; Gao, L.; Pu, Q.; Lu, J. J.; Wang, X. *J. Proteome Res.* **2006**, *5*, 323–329.

(28) Srinivasan, K.; Pohl, C.; Avladiovic, N. *Anal. Chem.* **1997**, *69*, 2798–2805.

(29) Razunguzwa, T. T.; Warriar, M.; Timperman, A. T. *Anal. Chem.* **2006**, *78*, 4326–4333.

(30) Towns, J. K.; Regnier, F. E. *Anal. Chem.* **1991**, *63*, 1126–1132.

(31) PQ Corp., Bulletin 12–31, 2003.

(32) Chirica, G.; Remcho, V. T. *Electrophoresis* **1999**, *20*, 50–56.

(33) Fields, S. M. *Anal. Chem.* **1996**, *68*, 2709–2712.

(34) Sakai-Kato, K.; Kato, M.; Homma, H.; Toyooka, T.; Utsunomiya-Tate, N. *Anal. Chem.* **2005**, *77*, 7080–7083.

(35) Lenza, R. F. S.; Vasconcelos, W. L. *Mater. Res.* **2001**, *4*, 175–179.



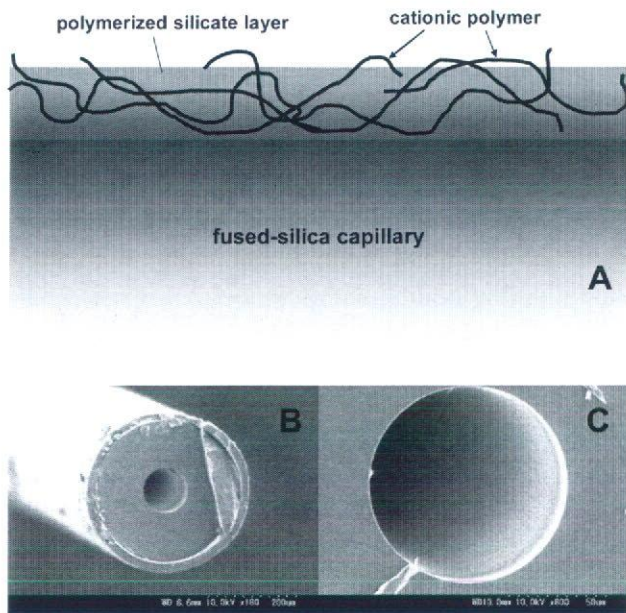


**Figure 1.** Schematic representation of cationic polymer entrapment in polymerized silicate (A). Scanning electron micrographs of the coated capillary (B and C). Capillary, 50  $\mu\text{m}$  i.d.  $\times$  360  $\mu\text{m}$  o.d.; coating, 1.5% PB in the coating mixture.

cationic polymers, such as PB. After the resulting mixture was pumped into the capillary, the excess removed and then allowed to dry, it yielded a stable coating, which we have named as KEIO (*Kasil-entrapped ionic*) polymer coating. Scanning electron micrographs showed that the coated layer was between 1.2 and 1.4  $\mu\text{m}$  in thickness (Figure 1B), and a “clean” surface was produced (Figure 1C). In X-ray diffraction studies of the structure of glass,<sup>36</sup> each silicon atom is tetrahedrally surrounded by four oxygen atoms, and part of the oxygen is bonded between two silicon and part to only one silicon. Although there is a distinct organization in the structure, there is no regular repetition in the pattern, resulting in a random silicon–oxygen network. The cationic polymer can be presumed to be entrapped within the various holes of the network.

**Characterization of the KEIO–PB Coating. (1) Effect of Polymer Concentration on EOF Mobility.** Similar to bare silica, the inner wall of the KEIO polymer-coated capillary intrinsically possesses negatively charged sites because of the presence of ionizable silanol groups. Incorporation of a positively charged polymer in the coated layer diminishes the net negative charge of the surface, which becomes progressively lower as the concentration of the polymer increases. At a polymer concentration that is high enough to supersede the effect of the silanols, the net charge of the surface becomes positive. The positive charge steadily increases as more polymers are incorporated until such point where further increases in polymer concentration no longer affect the resulting charge significantly.

Changes in surface charge will be reflected in the EOF. Figure 2 tracks the EOF as a function of the concentration of the cationic polymer PB in the coating mixture. The measurements were performed at pH 7, in which ionization of silanols was evident as well. In the absence of PB in the coating (i.e., a mixture of Kasil 1, water, and formamide only), a fast, normal (i.e., from anode to

cathode) EOF was generated. At low PB concentrations, the EOF remained cathode-directed, albeit becoming slower as the concentration of PB increased. At 0.1%, the EOF was reversed and then became faster with addition of more PB to the coating. At  $\sim$ 0.3%, the magnitude of the reversed EOF leveled off and was no longer significantly affected by further increases in PB concentration.

These results suggest that it is possible to manipulate the EOF in terms of both direction and magnitude by simply adjusting the concentration of the polymer in the coating. Thus, using KEIO–PB, the EOF can be tuned easily as may be required by the separation problem. In contrast, prior to commercialization of coating systems like CEofix<sup>37</sup> and EOfrol,<sup>38</sup> it is generally difficult to control the EOF in capillaries coated by conventional physical adsorption.<sup>39</sup>

**(2) Effect of Buffer pH on EOF Mobility.** The variation of EOF with pH under constant ionic strength conditions is represented graphically in Figure 3. In an uncoated capillary, the velocity of a cathodic EOF was clearly pH-dependent, i.e., high under neutral or alkaline conditions, reduced below pH 6, and significantly suppressed below pH 3. On the other hand, in a KEIO–PB(1.5%) capillary, a strong, anodic EOF was generated throughout the pH range 2–11, although it was slightly faster in the acidic region, where the ionization of silanols, which exert an effect counter to PB, was suppressed. In this manner, the pH can be varied to modify selectivity without considerably affecting the flow rate.

**(3) Stability.** The stability of KEIO–PB(1.5%) capillary was evaluated by monitoring the EOF in 300 successive runs, without any capillary conditioning except a 3-min high-pressure ( $\sim$ 940 mbar) rinse with the running buffer between consecutive analyses. Detachment of PB from the polymerized silicate is expected to be manifested as slowing down of the reversed EOF. The evaluation was performed at three pH values (pH 2.5, 4.5, and 8.5), and the results are shown in Figure 4. At pH 2.5 and 4.5, the EOF was practically unchanged over the 300-run course, thereby demonstrating the strong endurance of the coated capillary under acidic conditions. At pH 8.5, the EOF was initially slow and appeared to degrade faster, which could be attributed to the intrinsic instability of silicates at alkaline conditions. Regardless, the degradation, calculated to be  $\sim$ 22% at the completion of the 300th run, could still be considered reasonable, and stability was further improved by HMDS treatment of the coated capillary to protect the silanols prior to use (data not shown). While silicate itself is a strong adhesive and binder, which attaches the polymers tightly onto the wall, the long working lifetime of the coated capillary can also be attributed to the presence of polymeric additives all throughout the coating and not just on the surface. Thus, even if the outermost sections of the coating become unraveled from use, there are still polymers remaining in the next exposed level.

Addition of organic solvents to running buffers often expands the range of application of CE. Aqueous–organic solvent mixtures

(36) Warren, B. E.; Bischof, J. *J. Am. Ceram. Soc.* **1938**, *21*, 259–265.

(37) Lanz, C.; Marti, U.; Thormann, W. *J. Chromatogr., A* **2003**, *1013*, 131–147.

(38) Chang, W. P.; Nichols, L.; Jiang, K.; Schneider, L. V. *Am. Lab. News* **2004**, *36*, 8–13.

(39) Katayama, H.; Ishihama, Y.; Asakawa, N. *J. Chromatogr., A* **2000**, *875*, 315–322.



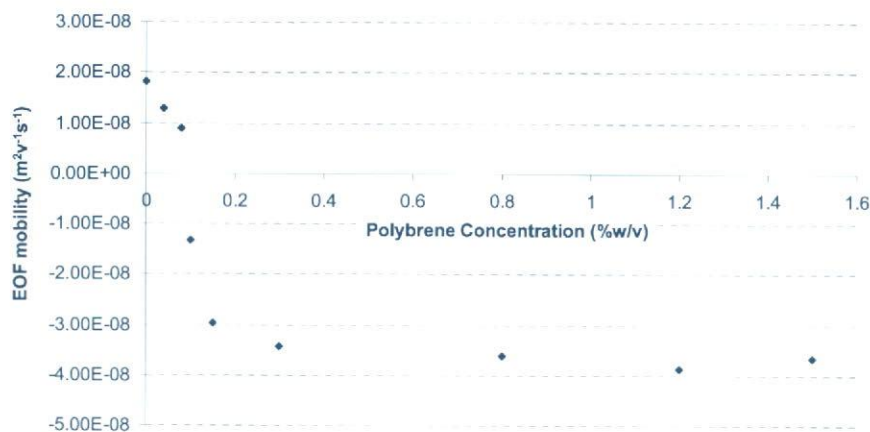


**Figure 2.** Dependence of EOF on concentration of PB in KEIO-PB capillaries. Conditions: capillary, 38.5 cm (30-cm effective length); background solution (BGS), 50 mM ammonium acetate, pH 7.0; applied voltage,  $\pm 20$  kV.

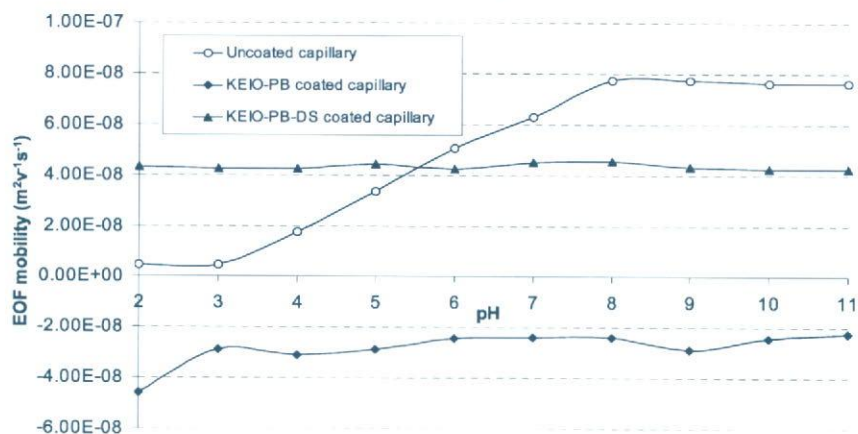


**Figure 3.** EOF vs pH profiles of uncoated, KEIO-PB(1.5%), and KEIO-PB(1.5%)-DS(3%) capillaries. Conditions: capillary, 38.5 cm (30 cm effective length); applied voltage,  $\pm 30$  kV.

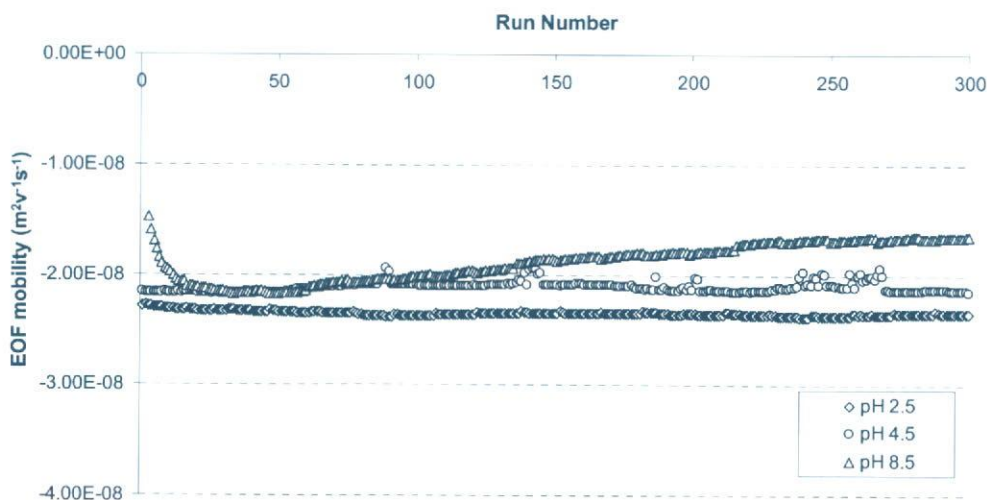


**Figure 4.** Endurance of KEIO-PB(1.5%) capillary. Conditions: capillary, 38.5 cm (30-cm effective length); applied voltage,  $-22$  kV.

may be used to modulate the EOF in order to widen the separation window, to increase the solubility of analytes, or to influence their acid-base properties. As such, for the coated capillary to be useful under practical conditions, it is imperative that it should also exhibit tolerance of these organic solvents. The EOF in KEIO-PB(1.5%) capillary was measured before and after 15-min, high-pressure rinses with some of the commonly employed organic solvents modifiers in CE (used herein as pure solvents), and stability was assessed on the basis of the degradation rate, as

shown in Table 1. As can be inferred from the results, degradation is minimal, which further attests to the stability of the coating.

KEIO-PB capillary was also tested against 1 M sodium hydroxide and 0.1 M hydrochloric acid. Being silicate-based, it showed poor tolerance of NaOH, and  $\sim 33\%$  reduction in EOF was observed in the run immediately following a 15-min rinse with the base. By comparison, after treatment with HCl, the capillary showed faster EOF. Such observation can be explained partly by a hysteresis effect and partly by a "polishing" effect of the acid;



**Table 1. Chemical Stability of KEIO–PB Capillary<sup>a</sup>**

	EOF <sup>b</sup> (m <sup>2</sup> V <sup>-1</sup> s <sup>-1</sup> ) (× 10 <sup>-8</sup> )	EOF <sup>c</sup> (m <sup>2</sup> V <sup>-1</sup> s <sup>-1</sup> ) (× 10 <sup>-8</sup> )	degradation rate (%)
methanol	2.15	2.13	0.56
acetonitrile	2.13	2.10	1.01
acetone	2.10	2.07	1.63
2-propanol	2.06	2.05	0.28
0.1 M HCl	2.05	2.40	(17.07) <sup>d</sup>
1 M NaOH	2.40	1.61	32.91

<sup>a</sup> Conditions: KEIO–PB(1.5%) capillary, 38.5 cm (30-cm effective length): BGS, 50 mM ammonium acetate, pH 4.5; applied voltage, –22 kV. <sup>b</sup> Measured EOF before a 15-min high-pressure rinse with solvent/solution. <sup>c</sup> Measured EOF after a 15-min high-pressure rinse with solvent/solution. <sup>d</sup> Please refer to explanation in text.

**Table 2. Run-to-Run and Coating-to-Coating Reproducibility<sup>a</sup>**

	EOF (m <sup>2</sup> V <sup>-1</sup> s <sup>-1</sup> ) (× 10 <sup>-8</sup> )	%RSD (n = 10)
capillary 1	2.16	0.84
capillary 2	2.13	0.73
capillary 3	2.33	0.90
capillary 4	2.24	1.43
capillary 5	1.95	0.49
coating-to-coating (n = 5)	2.16	6.48 (n = 5)

<sup>a</sup> Conditions are the same as given in Table 1.

i.e., it strips the outermost layer of the coating and exposes more of PB on the surface. This stripping is accompanied by removal of some PB as well; thus, coated capillaries treated with HCl and other acids, such as acetic acid and formic acid, evidenced slightly lower long-term stability than those that were not exposed to the same treatment.

**(4) Reproducibility.** Reproducibilities were assessed based on the relative standard deviations (RSDs) of the EOF obtained in 10 replicate runs, using 5 KEIO–PB capillaries from 5 independent preparations, and the results are shown in Table 2. The run-to-run RSDs were all within 1.5%, while coating-to-coating RSD was within 6.5%.

**KEIO–PB Capillary for Analysis of Anions.** CE analyses of anions are generally performed under reversed electrode polarity configuration,<sup>40,41</sup> such that the electrophoretic migration of the anions and the EOF are in the same direction, and the analyses can be completed within reasonable time. Using the same configuration in CE–MS, the reversed EOF must be adequately fast and constant to prevent deleterious current drops resulting from the formation of liquid gaps at the exit end of the capillary.<sup>42</sup> EOF reversal can be easily accomplished by addition of cationic modifiers to the running buffer; however, the overall stability of dynamic coating in CE–MS is less than that in CE with UV detection.<sup>42</sup> Accordingly, a capillary in which positive charges are stably fixed to the wall is preferred.

KEIO–PB capillary was employed in CE–MS analysis of some anionic metabolites included in the glycolytic, tricarboxylic acid,

**Table 3. Performance of KEIO–PB Capillary in CE–MS Analysis of Selected Anions (n = 5)<sup>a</sup>**

compound	m/z	peak area		migration time (min)	
		average (× 10 <sup>3</sup> )	RSD (%)	average	RSD (%)
glyoxylate	73	34	2.8	9.78	2.1
glycolate	75	64	3.1	9.47	2.0
pyruvate	87	81	4.0	9.40	2.0
lactate	89	128	3.1	10.19	2.2
fumarate	115	96	3.7	8.05	1.5
succinate	117	229	2.3	8.27	1.6
malate	133	133	6.4	8.25	1.6
2-oxoglutarate	145	161	2.4	8.26	1.6
phosphoenolpyruvate	167	132	3.0	8.38	1.3
dihydroxyacetonephosphate	169	182	5.0	9.47	2.0
glycerophosphate	171	302	3.7	9.63	2.0
3-phosphoglycerate	185	175	4.9	8.46	1.4
gluconate	195	374	4.2	12.19	2.7
erythrose 4-phosphate	199	153	2.4	10.09	2.2
ribose 5-phosphate	229	398	3.0	10.09	2.2
ribose 5-phosphate	229	539	2.9	10.27	2.0
glucose 1-phosphate	259 <sup>b</sup>	861	2.1	10.64	2.3
2,3-diphosphoglycerate	265	92	5.9	8.98	0.7
6-phosphogluconate	275	354	7.4	9.06	1.6

<sup>a</sup> Conditions: KEIO–PB(1.5%) capillary, 100-cm effective length; BGS, 50 mM ammonium acetate, pH 8.5; CE voltage, –30 kV; ESI voltage, –3.5 kV; injection, 30 s at 50 mbar; sheath liquid, 5 mM ammonium acetate in 50:50 methanol/water at 10 μL/min. <sup>b</sup> Data only on peak 1 are given because two compounds comigrated under peak 2.

and pentose phosphate pathways at pH 8.5, and good reproducibility of data on peak areas and migration times was obtained (Table 3; Supporting Information, Figure S1). It was applied successfully in the analysis of these compounds in the extract of fibroblast NIH 3T3 cells (Figure 5), as well as in rat plasma. The latter was prone to adsorb on the wall and block the charged, active sites; thus, the EOF progressively slowed down in the succeeding runs. However, by rinsing with 0.1 M HCl to flush out the adsorbed materials prior to conditioning with the running buffer, the EOF could be restored (Supporting Information, Figure S2).

In an uncoated capillary, enrichment of anions by prolonged electrokinetic injection is not very straightforward because, under alkaline conditions, the magnitude of the oppositely directed EOF is generally higher than the electrophoretic velocities of the anions. This necessitates the presence of a low-conductivity plug (e.g., water) prior to sample injection and careful monitoring of current for the requisite polarity switch. Using KEIO–PB capillary, field-enhanced sample injection of some anions could be carried out easily (Supporting Information, Figure S3), and more than 2000-fold improvement in detector response was obtained. The same configuration can be carried out using a neutral capillary. However, the use of KEIO–PB capillary has the potential of affording higher enhancement factors by exploiting the benefit of a similarly directed EOF, since the amount of ion injected depends on its velocity at the injection point, which in turn is the vector sum of its electrophoretic velocity and the EOF.

**Polymerized Silicate as a Base for Other Coatings.** Other cationic polymers can be similarly entrapped in polymerized silicate. For instance, KEIO–DEAE-dextran and KEIO–PEI capillaries were prepared easily, and these showed the same stability

(40) Romano, J.; Jandik, P.; Jones, W. R.; Jackson, P. E. *J. Chromatogr.* **1991**, *546*, 411–421.

(41) Jones, W. R.; Jandik, P. *J. Chromatogr.* **1991**, *546*, 445–458.

(42) Soga, T.; Ueno, Y.; Naraoka, H.; Ohashi, Y.; Tomita, M.; Nishioka, T. *Anal. Chem.* **2002**, *74*, 2233–2239.



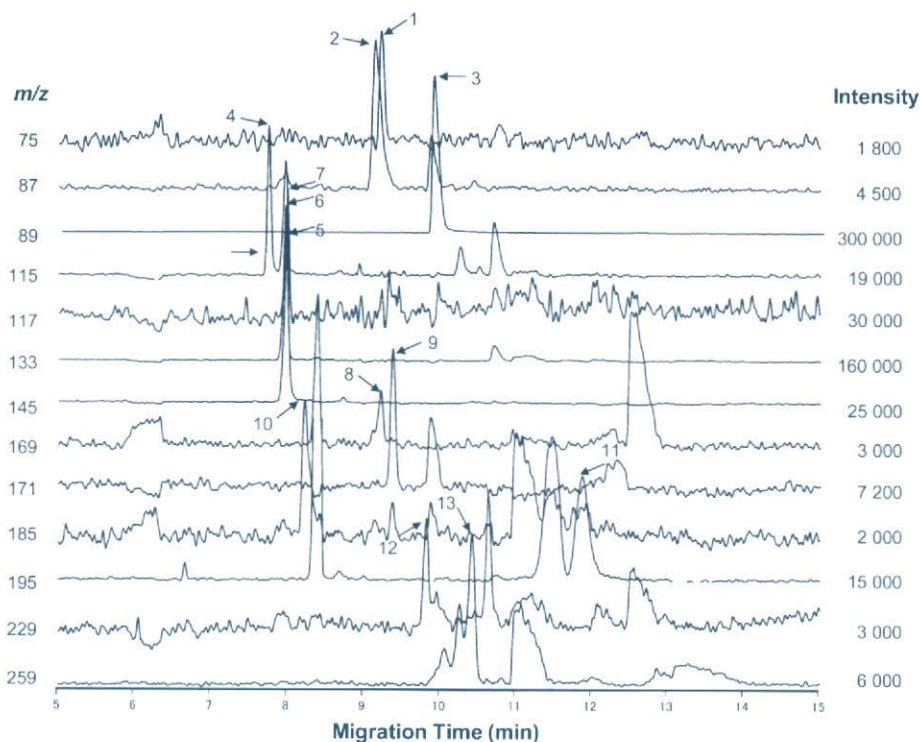


**Figure 5.** Some anionic metabolites found in the extract of fibroblast NIH 3T3 cells by CE-MS. Peaks (peak number,  $m/z$ ): glycolate (1, 73); pyruvate (2, 75); lactate (3, 89); fumarate (4, 115); succinate (5, 117); malate (6, 133); 2-oxoglutarate (7, 145); dihydroxyacetonephosphate (8, 169); glycerophosphate (9, 171); 3-phosphoglycerate (10, 185); gluconate (11, 195); ribose 5-phosphate (12, 229); fructose 6-phosphate and glucose 6-phosphate (13, 259). Intensity value indicated on the right-hand side refers to that of the most intense peak shown at the given  $m/z$ . Peaks were detected as their deprotonated ions. Conditions are the same as given in Table 3.

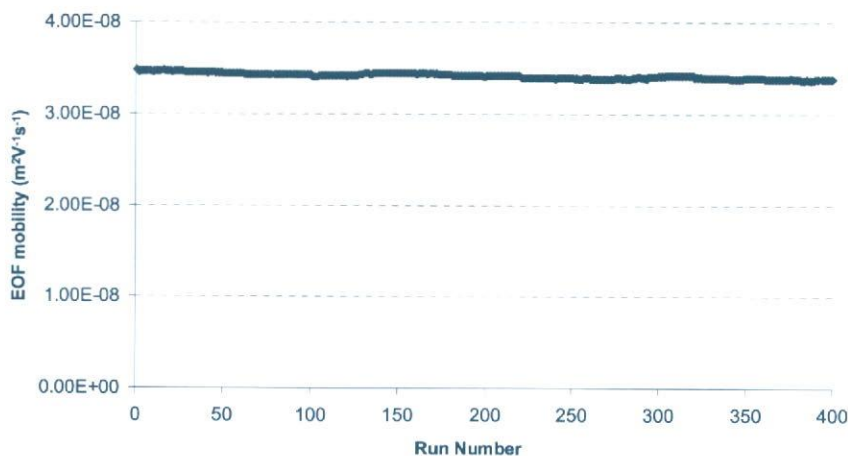


**Figure 6.** Endurance of KEIO-PB(1.5%)-DS(5%) capillary. Conditions: capillary, 38.5 cm (30-cm effective length); 50 mM phosphate, pH 2.5; applied voltage, 22 kV.

as KEIO-PB capillary, though, at the same polymer concentration (i.e., 1.5%), they exhibited slightly slower EOF. In particular, when KEIO-DEAE-dextran capillary was used under the same conditions for CE-MS analysis of anions as described previously, better separation performance was obtained, and the isomeric pair of ribulose 5-phosphate and ribose 5-phosphate ( $m/z = 229$ , partially overlapping in Supporting Information Figure S1,  $R_s = 0.8$ ) was baseline separated. Furthermore, fructose 6-phosphate and glucose 6-phosphate (comigrating under peak 2 at  $m/z = 259$  in Supporting Information Figure S1) were better resolved ( $R_s = 0.9$ ). KEIO-DEAE-dextran capillary was used continuously in more than 100 analytical runs of real samples without significant degradation in performance.

The KEIO-cationic polymer layer can also be used as a base for attaching anionic polymers on the wall, via electrostatic interaction with the cation in the primary layer. Using KEIO-PB(1.5%), we prepared DS(3%)-coated capillary, which showed a fast, pH-independent, cathodic EOF (Figure 3). KEIO-PB(1.5%)-DS(5%) capillary exhibited excellent endurance, with no appreciable change in EOF in 400 successive runs (Figure 6). By comparison, an equivalent capillary in which the primary layer was attached to the wall, using conventional physical adsorption method, endured only 100 runs.<sup>10</sup> The lower stability of the previous two-layer coating scheme made up of successive layers of oppositely charged polymers was thought to be due to the weak attachment of the inner layer of cations to the silica surface. Thus,

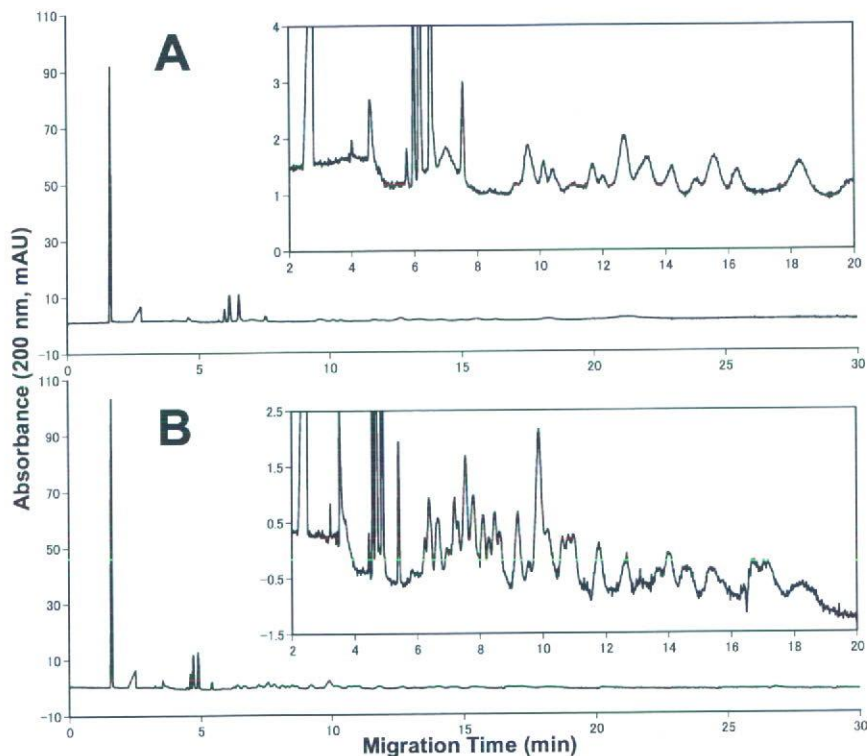


**Figure 7.** CE analyses of tryptic digest of pig serum albumin using KEIO–PB(1.5%) (A) and KEIO–PB(1.5%)–DS(3%)–PB(10%) (B) capillaries. Conditions: capillary, 58.5 cm (50-cm effective length); BGS, 100 mM phosphate, pH 2.0; injection, 5 s at 50 mbar of 5 pmol/ $\mu$ L digest; applied voltage, –30 kV. Insets show expanded views of the electropherograms between 2 and 20 min.

when this was supplanted with silicate-stabilized cations, the overall stability of the coating was improved. KEIO–PB(1.5%)–DS(5%) capillary was also evaluated for its tolerance of common organic solvents, namely, methanol, acetone, acetonitrile, 2-propanol, and ethanol, as well as 0.1 M HCl, and 1 M NaOH in a manner similar to that described for KEIO–PB. It showed no remarkable change in EOF (i.e., degradation rates were all less than 0.2%) in the runs following high-pressure rinses with any of the abovementioned solvents or solutions. The RSDs of the observed EOF mobility in 10 replicate runs from 5 independent preparations were all better than 0.4%, while the coating-to-coating RSD was within 4.1%. KEIO–PB(1.5%)–DS(5%) capillary showed good performance in the analysis of acidic proteins at physiologic pH, as well as in rapid micellar electrokinetic chromatography-sodium dodecyl sulfate analysis of benzene derivatives at low pH and normal polarity (Supporting Information, Figure S4).

The capillary was further developed by adding a third layer, consisting of cationic polymers adsorbed on the surface of the second layer (KEIO–PB(1.5%)–DS(3%)–PB(10%)). Whereas a one-layer coating has been demonstrated as adequate for small molecules, the presence of unmasked silanols impaired the performance of the capillary for those with tenacious affinity for them, e.g., peptides. Therefore, it was necessary to attach a third layer of PB to more effectively shield the silanols and obtain better results. Figure 7 compares the performance of KEIO–PB(1.5%) and KEIO–PB(1.5%)–DS(3%)–PB(10%) capillaries in the analysis of a tryptic digest of pig serum albumin at low pH. Faster migration times of the peptides in the latter suggest higher density of PB

on the surface and presumably better shielding of silanols; thus, sharper peaks were observed.

## CONCLUSION

A new, facile strategy for preparing coated capillaries based on polymer entrapment in polymerized silicate was developed. The KEIO–polymer coated capillaries have strong endurance thereby ensuring their long working lifetimes, while their good stability over a wide range of pH and chemical tolerance enables their effective utilization under diverse separation conditions. The coating technique has been demonstrated herein using a conventional capillary format. However, the ease with which the procedure can be carried out makes it easily exportable to the chip format as well.

## ACKNOWLEDGMENT

The authors gratefully acknowledge PQ Corporation for the gift of potassium silicate solution, Sachie Sato, Satsuki Ikeda, Yasuyuki Igarashi, and Yuji Kakazu of IAB for technical assistance, and Shota Miyazaki of GL Sciences for the SEM images of the coated capillary. We also thank Prof. Takaaki Nishioka of IAB for support and fruitful discussions.

## SUPPORTING INFORMATION AVAILABLE

Additional information as noted in text. This material is available free of charge via the Internet at <http://pubs.acs.org>.

Received for review May 21, 2007. Accepted July 30, 2007.

AC071038Y



Review

# Metabolome analysis by capillary electrophoresis–mass spectrometry

Maria Rowena N. Monton<sup>a</sup>, Tomoyoshi Soga<sup>a,b,\*</sup>

<sup>a</sup> Institute for Advanced Biosciences, Keio University, Tsuruoka, Yamagata 997-0017, Japan

<sup>b</sup> Human Metabolome Technologies Inc., Tsuruoka, Yamagata 997-0017, Japan

Available online 24 February 2007

## Abstract

Capillary electrophoresis (CE)–mass spectrometry (MS), as an analytical platform, has made significant contributions in advancing metabolomics research, if still limited up to this time. This review, covering reports published between 1998 and 2006, describes how CE–MS has been used thus far in this field, with the majority of the works dealing with targeted metabolite analyses and only a small fraction using it in the comprehensive context. It also discusses how some of the key features of CE–MS were exploited in selected metabolomic applications.  
© 2007 Elsevier B.V. All rights reserved.

**Keywords:** Metabolome analysis; Metabolomics; CE–MS

## Contents

1. Introduction .....	237
2. Technical considerations .....	238
2.1. CE .....	238
2.2. MS and interfaces .....	239
2.3. CE–MS for comprehensive analyses .....	240
3. Selected applications .....	242
3.1. Sample characterization .....	242
3.2. Elucidating metabolic dynamics .....	243
3.3. Assigning functions to genes and proteins .....	243
3.4. Disease diagnosis and biomarker discovery .....	243
3.5. Assessing food safety .....	245
4. Conclusions and future outlook .....	245
References .....	245

## 1. Introduction

“Metabolomics” is the newest “omics” buzzword in the field of systems biology, joining genomics, transcriptomics and proteomics. The “metabolome,” the complete set of small (typically less than 1 kDa) molecules (metabolites) present in cells in a particular physiological or developmental state [1],

is said to be closest to the phenotype; thus, metabolomics is poised to play a critical role in understanding intricate biochemical and biological systems. Metabolites are not organism-specific; hence, a single approach for a particular metabolite or metabolite class can be adopted regardless of the species being interrogated [2]. Moreover, their number is projected to be less than those of genes and proteins [1,3]. Despite these, metabolome analysis presents a primary analytical challenge because the wide diversity of metabolites in terms of physico-chemical properties and abundance make their simultaneous determination difficult [4–8]. They can range from small inorganic ions to hydrophobic lipids and complex natural products, and occur in widely diverging concentrations,

DOI of original article: [10.1016/j.chroma.2007.02.067](https://doi.org/10.1016/j.chroma.2007.02.067).

\* Corresponding author at: Institute for Advanced Biosciences, Keio University, Tsuruoka, Yamagata, Japan. Tel.: +81 235 29 0528; fax: +81 235 29 0574.

E-mail address: [soga@sfc.keio.ac.jp](mailto:soga@sfc.keio.ac.jp) (T. Soga).



spanning over nine orders of magnitude (from pmol to mmol) [7].

Given that the ultimate goal of metabolomics is to identify and quantify *all* metabolites in a given system in an unbiased, reproducible way [2], there is no single analytical methodology that is currently available, which is capable of doing so [2,4–8]. Thus, metabolomics, in the strictest sense, is practically impossible, and the term is used broadly to cover approaches concerned with investigating subsets of the metabolome. These approaches include metabolite profiling, target analysis, metabolite fingerprinting and metabolite footprinting [2,5–9]. Metabolite profiling involves identification and quantitation of a group of metabolites common to a specific pathway or chemical class. Target analysis is even more exclusive in that it focuses only on a particular metabolite or metabolite class. In contrast, metabolite fingerprinting and footprinting involve rapid, comprehensive analysis of samples, generally for the purpose of observing signature patterns, i.e., “fingerprints” or “footprints” (i.e., extracellular metabolites, such as those in spent culture media), without necessarily identifying nor quantifying individual metabolites.

Metabolomics draws on a range of analytical platforms including nuclear magnetic resonance (NMR) spectroscopy, mass spectrometry (MS), and chromatography- and electrophoresis-based separation methods. NMR is an attractive technique for high-throughput fingerprinting and profiling studies as it does not require extensive sample preparation, is non-destructive and can uniformly detect all compounds with NMR-measurable nuclei [10]. Its principal drawbacks, however, are its poor sensitivity and high sample requirement. MS, on the other hand, affords high sensitivity and selectivity, but it can discriminate against some compound classes, depending on the type of ionization used. NMR and MS may be employed as stand-alone techniques; however, it is generally regarded that strategic matings with upstream separation methodologies enhance their performance for complex mixtures.

Practical issues in interfacing gas chromatography (GC) and liquid chromatography (LC) with MS were resolved early on; hence, they are considered as mature technologies. GC–MS, in particular, is a mainstay in plant metabolomics [11]. A significant development in GC in the last decade is comprehensive, two-dimensional GC (GC  $\times$  GC). Generally, the sample components are separated in the first column according to their volatilities, then small fractions of the effluent are trapped and focused using a modulator, and sequentially released into the second column for further separation, this time, based on polarity differences [12]. GC  $\times$  GC offers much greater peak capacities, and with high-speed time-of-flight (TOF)-MS as detection method, it is good for complex samples [13,14]. GC, however, is limited to volatile metabolites and those that can be derivatized to yield volatile, thermostable products. In contrast, LC is more rugged and amenable to more types of compounds. Whereas traditionally regarded as inferior to GC in terms of separation efficiency, recent technology advancements in LC have resulted in improved performance. For instance, innovations in pump systems enable operations at elevated pressures, and led to the development of the so-called ultra-performance LC (UPLC).

With particles less than 2  $\mu\text{m}$  packed in long capillary columns, fast analyses with as high as 300,000 plates can be obtained [15]. UPLC-MS is used increasingly in metabolomic applications [16,17]. Still, a large number of metabolites are too polar to be significantly retained by reversed-phase columns that are commonly employed [18]. Since a major fraction of metabolites are polar and ionic, a good approach is to use capillary electrophoresis (CE)–MS. In contrast with GC and LC, which operate based on differential interaction with a stationary phase, CE separates analytes according to their mass-to-charge ratios. This orthogonality in separation principle underscores the relevance of CE as a complementary tool to the more established chromatographic techniques—in many cases, samples that cannot be easily resolved by GC or LC can be separated by CE. Fast, highly efficient separations, without requiring rigorous sample pretreatment, can be obtained, and running costs are low. The most attractive feature of CE, though, is its small sample requirement (a few nanoliters at most), making it particularly well-suited for samples that are volume-limited. Poor concentration sensitivity, which is often cited as a disadvantage of CE when fitted with absorbance-related detectors, does not pose a significant problem with MS for detection. Additionally, it is possible to perform facile in-capillary sample enrichment schemes to boost sensitivity [19–22], without the need for dedicated instrumental modifications, when necessary. Thus, CE–MS represents a viable platform for metabolomic studies. To date, however, reports based on CE–MS constitute only a small fraction, with most of these dealing with targeted metabolite analysis, and only a few in the context of comprehensive metabolome analysis. In this review, we describe how CE–MS has been applied thus far in the field of metabolomics, and discuss how some of its key features were exploited in selected applications.

## 2. Technical considerations

### 2.1. CE

CE is a versatile technique which is able to separate a wide range of analytes, from small inorganic ions [23] to large proteins [24] and even intact bacteria [25]. By simply incorporating additives (e.g. micelle, chiral selector, complexing agent) into the run buffer, a variety of separation formats can be explored. But because of buffer component constraints when coupling with MS via electrospray ionization (ESI), the most common interface, its simplest form, i.e., capillary zone electrophoresis (CZE), is utilized, with few exceptions. Micellar electrokinetic chromatography (MEKC), a powerful mode for separating neutrals based on partitioning to charged micelles, cannot be combined with MS in a straightforward way because micelles tend to contaminate the ion source, suppress analyte ionization, and decrease MS response. To prevent sensitivity losses, modifications on the MEKC side have been adopted, including the use of volatile [26] and high molecular weight micelles [27], and the so-called partial filling (PF) technique [28], in which separation is effected only in a limited section of the capillary filled with micellar solution. As demonstrated by Frommberger et al. [29], *N*-Acyl-L-homoserine lactones (AHLs), a class of micro-



bial signaling molecules with no chargeable group, could be separated by PF-MEKC-MS, using, at most, 80% of the total capillary length for micellar separation, and two AHLs from *Burkholderia cepacia* colonizing the rhizosphere of traditional Indian rice cultivars could be unambiguously identified. The difficulty with such an approach, however, is that separation performance is often compromised. Thus, interfacing via alternative ion sources [atmospheric pressure chemical ionization (APCI) and atmospheric pressure photoionization (APPI)], while leaving the separation conditions intact, have also been carried out (further discussion on APCI and APPI can be found in Section 2.2).

Derivatization imparts more suitable characteristics to the analytes of interest. It is generally detection-oriented, associated with the incorporation of functional groups to the molecules for enhanced detection sensitivity [30]. In some cases, derivatized moieties can be resolved better. Che et al. [31] subjected dextran to acid hydrolysis, and the hydrolysate was derivatized with 8-aminonaphthalene-1,3,6-trisulfonate (ANTS) by reductive deamination. This introduced negative charges to the oligosaccharides, which facilitated their migration in an electric field. Larsson et al. [32] adopted the same technique for maize starch oligosaccharides, enabling their separation as anions even at low pH conditions. In the preceding examples, the derivatization step was completed prior to sample injection. In a different strategy, Ptolemy et al. [33–35] performed this step within the capillary via zone passing of a concentrated plug of the derivatizing reagent during electromigration. Since derivatization also alters the migration behavior of analytes, this has the additional benefit of enabling sample preconcentration, thereby increasing sensitivity. This technique was applied in analyses of bacterial biomarkers and in fundamental metabolic flux studies in *Escherichia coli* cell cultures.

CE buffers are generally aqueous-based, though nonaqueous systems are exploited as well, particularly for analytes that are insoluble or sparingly soluble in water. Moreover, they permit some hydrophilic interactions, such as hydrogen-bonding, dipole-related and ionic interactions, which are thermodynamically strengthened in hydrophobic environment, to be explored better [36]. When hyphenated with MS via ESI, nonaqueous CE (NACE) circumvents buffer compatibility problems, and even enhances sample ionization process which results in improved detection limits compared to separation in aqueous buffer systems [37]. Bianco et al [38] used NACE to determine glycolalkaloids in *Solanum tuberosum* (potato), and the results were found to be comparable to those obtained using LC-MS. In a follow-up work [39], they utilized the system they developed for comparing the glycoalkaloidal content of transgenic and wild type potato tubers. Sturm et al. [40] and Unger et al. [41] used NACE to determine isoquinoline alkaloids in *Fumaria officinalis* and related phytopharmaceuticals, and naphthylisoquinoline alkaloids in crude extracts from an African *Ancistrocladus* species, respectively. Vuorensola et al. [42] analyzed catecholamines in both aqueous and alcoholic nonaqueous solutions, and found that their separations were more efficient in nonaqueous media than in water.

## 2.2. MS and interfaces

ESI and matrix-assisted laser/desorption ionization (MALDI) are the most common MS interfaces for biomolecular analyses. ESI enables direct transfer of molecules from the liquid phase to the gas phase [43]; hence, it can be more easily adapted for on-line hyphenation of MS with CE, as well as LC. In contrast, approaches integrating MALDI are essentially off-line [44–46], since it requires a solid matrix. MALDI is a popular technique for proteomics, but it is not as widely employed in metabolomics because of the strong interference from matrix ions in detection of low molecular weight compounds [47].

CE-ESI-MS designs should provide a means for completing the CE electrical circuit for analyte separation, while simultaneously providing an electrical potential to the spray tip. This is generally accomplished using sheath-flow or sheathless interfaces. The first is the most common approach by far because of its robustness and the ease with which it can be implemented. In such configuration, a coaxial sheath liquid, generally a hydroorganic mixture, mixes with the effluent at the exit end of the capillary. Its flow rate and composition can be varied to optimize detection. Several reports have indicated that the type and proportion of organic solvent and volatile acids (e.g., acetic acid and formic acid in the positive ion mode) and bases (e.g., ammonia and trimethylamine in the negative ion mode) affect the intensity of MS signals [48–54] and even influence resolution [55]. For instance, García-Villalba et al. [52] showed that the use of 50:50 v/v 2-propanol/water with 0.1% v/v triethylamine gave the highest signals for the negative ion mode detection of hop acids. On the other hand, Li et al. [53] reported that a pure organic sheath solution (i.e., a mixture of 2-propanol and methanol) offered better stability and sensitivity for lipopolysaccharides (LPS) in *Neisseria meningitidis*. More importantly, it was compatible with both negative and positive ion mode detections, permitting the use of polarity switching in a single CE run.

To ensure a stable electrospray, the sheath liquid is usually introduced at a higher flow rate than the capillary effluent [43]. Because dilution occurs at the mixing point, sensitivity tends to be compromised. This problem can be avoided with sheathless interfaces. Several designs are available, but technical difficulties in configuring them have largely precluded their routine use. Edwards et al. [56] fabricated an electrically porous junction by etching a short section of the capillary with hydrofluoric acid (Fig. 1). The concentration and mass detection limits they obtained averaged 7- and 5-fold lower than those previously reported for some *E. coli* metabolites in CE-MS using a sheath-flow system [57]. Zamfir et al. [58] butted the separation capillary to a commercial nanospray needle via an in-house assembled joint, and ESI voltage was applied to the needle using a stainless steel clenching device. This CE-nanoESI-MS system was applied to the systematic screening of complex oligosaccharide mixtures, permitting detection in the pmol level. Schultz and Moini [59] used a split-flow technique, in which a small hole was drilled near the capillary outlet, through which a small percentage of the capillary effluent exited and contacted a metal tube acting as the CE outlet/ESI shared electrode. Its